Abstract

BELYEA, JENNIFER LEE. Spectroscopic Characterization of the Function and Mechanism of Dehaloperoxidase. (Under the direction of Stefan Franzen)

The research presented in this thesis focuses on three main areas of work with dehaloperoxidase, DHP. The development of a viable source of recombinant DHP is discussed first. Enzymatic activity of DHP is the second area of research discussed followed by ligand binding studies. All of this research is done in the attempt to understand the structure function relationship within DHP. DHP's globin structure and peroxidase activity is the source of our interest in studding the structure function relationship in DHP. Typically, globins are not peroxidases. In DHP's case a unique heme active site, that is not common for globins or peroxidases, alters the ligand binding and the Poulos-Kraut push/pull mechanism of compound I formation. Specifically DHP has a distal valine residue that is unable to function as the residue that is responsible for the abstraction of a proton. Typically, the distal residue in both globins and peroxidases is a histidine. The distal histidine is credited with the abstraction of the proton in the pull step of the Poulous-Kraut push/pull mechanism.

# SPECTROSCOPIC CHARACTERIZATION OF THE FUNCTION AND MECHANISM OF DEHALOPEROXIDASE

by

**JENNIFER LEE BELYEA**

A thesis submitted to the Graduate Faculty of
North Carolina State University
in partial fulfillment of the requirements
for the Degree of
Masters of Science

**DEPARTMENT OF CHEMISTRY**

Raleigh, North Carolina

June 2004

**APPROVED BY**:

| | |
|---|---|
| _____ | _____ |
| Dr. Edmond Bowden | Dr. Steven Lommel |

_____
Dr. Stefan Franzen
Chair of Advisory Committee

## Dedication

This work is dedicated to my family. My parents have always been my cheerleaders encouraging me to do to my best and keeping my sprits up when thing did not work out as I desired. My sister has become much more than a source of spare parts she is a driving force that pushes me to better myself as a person. My husband is my greatest source of support, if it were not for Curtis none of this work would have been possible. Curtis has helped me with each and every experiment, task, frustration and accomplishment. I am grateful to be part of such as supportive family.

## Biography

Jennifer Lee Belyea was born on June 24, 1976 in Singapore, to Charles and Lek Lek Browning. Jennifer grew up with a younger sister, Carol Sui, in West Plains Missouri where she attended West Plains High School. After High School, Jennifer attended the University of Missouri in Columbia Missouri where she received a B.S in Chemistry.

Acknowledgements

I would like to thank my advisor, Stefan Franzen, for the opportunity to work in his laboratory and the chance to work with dehaloperoxidase. Thanks to Drs. Bowden and Lommel for the opportunity to work in their laboratories. Thanks to Dr. Tim Sit for the help and his patience with the cloning work. Thanks to Dr. Clay Clark and his lab for the use of their stopped-flow apparatus. Thanks to Dr. Martin Vos for his work with the NO recombination experiments. I would like to thank Marisha Godek, Lauren Collins and Robin Casey for their help getting this project of the ground. Thanks to Scott Brewer and Dr. Simon Lappi for their help with instruments and advice. Special thanks to Mike Davis and Lauren Gilvey for their interest in this project and willingness to work on and finish much of what has been started. Thanks to Curtis Belyea for all the clean glassware, solutions, labor, and his tolerance for my nights and weekends in lab.

# Table of Contents

# List of Tables

Page

# LIST OF FIGURES

Page

# Chapter 1: Introduction and Background

## 1.1 Introduction and Background

Dehaloperoxidase (DHP) is an enzyme isolated from the marine worm *Amphitrite ornata*[1-6]. In the presence of peroxide and a suitable substrate such as tribromo-, trichloro- or even trifluorophenol, DHP catalyzes the oxidation of the phenol to a quinone product[1]. The exact nature of the product distribution has not been determined, but assays show that the reactivity is similar to horseradish peroxidase[7]. None of this would be remarkable if not for the fact that the structure of DHP is nearly isomorphous with known myoglobin structures, and known globins have essentially no peroxidase activity[1,4]. This makes DHP the first known peroxidase with a globin fold and in fact, only the second enzyme known to have a globin fold[3]. Due to the structural homology with globins and activity as a peroxidase, dehaloperoxidase is an ideal enzyme to probe the structure/function relationship of proteins.

Until now, all of the studies of DHP have been carried out using protein isolated from *A. ornata*. Even though there is an X-ray crystal structure of the enzyme with a bound substrate analog (4-iodophenol), the proof that DHP is the enzyme required farther characterization[5]. The characterization of the mechanism and dynamics of this enzyme is a central target of the work in this thesis. Several spectroscopic studies were developed to understand the mechanism of DHP. The protein initially had to be isolated from the worm[1-6]. It is not convenient to obtain large amounts of protein by this method therefore the first barrier that had to be over come was the lack of protein.

## 1.2 Cloning, Expression and Purification of DHP and 6x His DHP

The spectroscopic studies undertaken in this thesis require large amounts of protein. For this reason the initial phase of this project is devoted to the cloning expression and purification of DHP protein in *E. coli*. The cloning and expression have the further

advantage in that, site-directed mutants could be expressed and studied as well[9]. Recombinant forms of dehaloperoxidase are isolated as a stable oxyferrous dimmer of 31kD.

**1.3 Assays Involving DHP and 6x His DHP**

With a source of recombinant dehaoperoxidase the activity of the enzyme is tested to ensure that the recombinant protein behaves like the wild type dehaloperoxidse. UV-Vis assay data in this section suggests that dehaloperoxidase does not use peroxide as a cosubstrate. Our conclusion, therefore, is that there must be an alternative mechanism to generate compound I.

**1.4 CO Recombination as a Function of Temperature**

Fourier transformed infrared (FTIR) spectroscopy is used to further characterize the recombinant dehaloperoxidase. Similar Fourier transformed infrared experiments on native dehaloperoxidase have resulted in similar results to those shown in chapter four of this thesis. Do to a greater availability of recombinant protein; we have expanded the sample conditions to include different pHs and presence of substrate. In this section Fourier transformed infrared data shows shifts in A and B states due to pH and the presence of substrate, 2,4,6-tribromophenol. This method, FTIR, has provided the only means of a direct comparison of the recombinant and native forms of dehaloperoidase.

**1.5 Effects of Glycerol Concentration on NO Ligand Recombination**

Picosecond Transient absorption experiments measuring the effects of glycerol concentration on NO ligand recombination were performed at the Laboratorie d'Optique et Biosciences located at Ecole Palaiseau, in France. This study shows that the presence of substrate has the same effect as increased viscosity on ligand recombination. This data can be used to further modify the push-pull mechanism of dehaloperoxidase's activity discussed

in Chapter 2. Similar studies have been done on myoglobin and mutants of myoglobin. Dehaloperoxidase is a structural homolog to the sperm whale myoglobin mutant H64V. In H64V the 64$^{th}$ residue a histidine, that was mutated to a valine. Dehaloperoxidase has a valine in the same position thus DHP was compared to H64V.

## References


1. LaCount, MW., Zang, EL., Chen, YP., *et al*. The crystal structure and amino acid sequence of dehaloperoxidase form *Amphitrite ornata,* indicate common ancestry with globins, Journal of Biological Chemisty 2000; 275: 18712 – 18716.
2. Zhang, E., Chen, YP., Roaach, MP., *et al*. Crystallization and initial spectroscopic characterization of the heme-containing dehaloperoxidase from the marine polychaete *Amphitrite ornata,*. Acta Cryst. 1996; **D52**: 1191-1193**.**
3. Roach, MP., Chen, YP., Dawson, JH., *et al*. *Notomastus lobatus* Chloroperoxidase and *Amphitrite ornata,* Dehaloperoxidase both contain histidine as their proximal heme iron ligands, Biochemistry 1997; **36**: 2197-2202.
4. Lebioda, L., LaCount, MW., Woodin, SA., *et al* An enzymatic globin from a marine worm Nature 1999; **401**: 445
5. Chen, YP., Woodin, SA., Lincoln, DE., and Lovell, CR., An unusual dehalogenating peroxidase from the marine terebellid polychaete *Amphitrite ornata,* The Journal of Biological Chemistry 1996; **9**: 4609-4612.
6. Han, K., Woodin, SA., Ely, B., *et al*. *Amphitrite ornata,* a Marine Worm, Contains Two Dehaloperoxidase Genes, Marine Biotechnology 2001; **3**: 287-292
7. Hewson, WD., Dunford, HB., Oxidation of p-Cresol by Horseradish Peroxidase Compound I, The Journal of Biological Chemistry. 1976; **19**: 6036-6042
8. H. Brian Dunford, Heme Peroxidases, Wiley-VCH, New York, 1993

# Chapter 2: Cloning, Expression and Purification of DHP and 6x His Tagged DHP

## 2.1 Introduction

The goal of the work presented in this chapter is to clone DHP in order to provide an abundant and independent source of protein. Until now, studies concerning DHP have been completed using protein isolated from *A. ornata*. The native form of protein is not abundant and may contain contaminates. Protein isolated from the marine worm way have one or more contaminates that possess the true peroxidase activity observed; thus, a non native source of protein is an ideal approach to eliminate contaminates and to provide an abundant source of protein.

In the following chapter, the cloning, expression and purification of DHP is documented. The major obstacle to the expression of DHP in *E. coli* is the presence of the codon, AGG, in the *A. ornata* gene for dehaloperoxidase that is not read by the *E. coli* translational apparatus. To overcome this obstacle, cloning of the dehaloperoxidase gene into a "Rosetta" cell line that contains all the tRNAs utilized in the DHP gene sequence is described[7].

## 2.2 Materials and Methods

*Cloning of the DHP gene into the Rosetta (DE3) pLysS cell line:*

The DHP coding region was amplified from a cDNA construct with *PfuTurbo*® DNA polymerase (Stratagene, La Jolla, CA) using primers that incorporated a unique *Nco*I site at the amino terminus (5'TATTACCATGGGGTTTAAACAAGATATTGC) and a *Bam*HI site at the carboxyl terminus (5'TATTAGGATCCTACTTCATGCCTGCGCTGC). An alternate 5' primer coding for an additional 6 His residues (bold typeface; 5'TATTACCATGGGG**CACCACCACCACCACCAC**TTTAAACAAGATATTGC) was

also used to produce a 5' Histidine-tagged DHP for ease of purification on Ni-NTA columns. A Stratagene RoboCycler Gradient 96 thermacycler was used to conduct all the PCR's with the following program for the amplification of the DHP gene coding for both His tagged and non His tagged proteins; window 1: 94$^{o}$C for 3 minutes 47-58$^{o}$C for 1 minute then 72$^{o}$C for 90 seconds 2 cycles, window 2: 94 $^{o}$C for 45 seconds 47-52$^{o}$C for 45 seconds and 72$^{o}$C for 80 seconds 38 cycles, window 3 72$^{o}$C for 10 minutes 1 cycle, window 4 cools to 6$^{o}$C. The amplified DNA were purified using QIAprep Miniprep kits (Qiagen, 27104).

Complementary nucleotide overhang ends on the DHP amplification product and the pET-16B plasmid were generated using Bam HI (New England Biolabs, R0136S) and Nco I (New England Biolabs, R0193S) for ligation in to the pET-16B vector. After ligation of the DHP gene into pET-16B the vector was heat shocked into DH5α competent *E. coli* cells. Plasmids were isolated from the DH5α cells using QIAprep Miniprep kits (Qiagen, 27104).

*Expression of the DHP Enzyme from the pET-16b expression vetor:* 6XHis and unmodified sequence in Rosetta (DE3) pLysS were stored as glycerol stocks in a –70 $^{O}$C freezer. The glycerol stock was used to streak a 2XYT agar plate supplemented with ampicillin and chloramphenicol. The plate was incubated overnight at 37 $^{o}$C. 2XYT media containing ampicillin and chloramphenicol was inoculated with several colonies. The cultures were allowed to grow at 37 $^{o}$C for 10 to 16 hours then were centrifuged in a Sorvall RC-5B using 250 ml bottles at 8000 X g (7,000 rpm with a KA-10 rotor) for 10 minutes. No induction was necessary. After centrifugation the cell pellet was collected and frozen in a -20 $^{O}$C freezer until purification.

*Purification of 6X-His tagged Dehaloperoxidase from Rosetta (DE3) pLysS:*

A cell pellet weighting 50 g was removed from a –20$^{O}$C freezer and allowed to thaw

in 10 ml of lysis buffer (50 mM $NaH_2PO_4$, 300 mM NaCl, 10 mM imidazole, pH 8.0) per gram wet weight of cell pellet for 15 minutes. Once cells were thawed, they were resuspended by stirring at 4 $^oC$ for 10 minutes. After resuspension, lysozyme was added to a final concentration of 1 mg/ml and incubated on ice for 30 minutes. After incubation with lysozyme, the cell mixture was sonicated in a Fisher Scientific FS20 sonicator for 30 minutes in an ice water bath. RNase A and DNase I were added to the viscous lysate resulting in a final concentration of 10 µl/ml and 5µl/ml, respectively. The lysate was allowed to incubate on ice for 15 minutes, before being centrifuged at 10,000x g for 30 minutes at 4 $^oC$ (KA-21.5, 9,250 RPM).

The purification of the 6X His tagged protein was done using Ni-NTA agarose (QUIAGEN Cat.No. 30210). The procedure was modified from Qiagen's manual which accompanies the Ni-NTA agarose. The lysate, which was translucent red in color, was loaded onto the column. The effluent was translucent with an orange tint. When the lysate, was loaded the wash buffer (50mM $NaH_2PO_4$, 300 mM NaCl, 20 mM imidazole, pH 8.0) was applied at 3 times the column volume. The elution buffer (50 mM $NaH_2PO_4$, 300 mM NaCl, 250 mM imidazole, pH 8.0) was then added to the column. Fractions were collected according to the intensity of the color of the eluted protein solution. Once the column was completely eluted, the fractions were analyzed by SDS-PAGE and by UV-vis spectroscopy. Fractions that had a purity number (ratio of Soret absorbance to absorbance at 280 nm) of 2.5 or greater were pooled. The pooled fractions were concentrated by Amicon centriprep YM-10 (4321). The concentrated protein solution was then used for assays.

*Purification of Dehaloperoxidase from Rosetta (DE3) pLysS:*

A 50 g cell pellet was thawed and suspended by stirring in a minimal amount of lysis buffer (50 mM Tris, 100 mM NaCl, 5 mM EDTA; 4 ml per gram of cell pellet) for 30 minutes at 4 $^{o}$C. After stirring, the cell solution was refrozen with liquid nitrogen or dry ice until completely solid. The red color of the frozen cell solution intensified upon freezing. The cells were then thawed in a 37 $^{o}$C oven. This solution was centrifuged for 20 minutes at 26,892 X g (KA-21.5, 15000 RPM with 50 ml centrifuge tubes). After centrifugation the supernatant and pellet were collected separately.

Heme biosynthesis lagged behind the synthesis of the protein; therefore, heme was added to the apo-protein to maximize yield. The pellet was resuspended in a minimal amount of lysis buffer and 40 µl of heme solution per gram of original cell pellet. The cell mixture was allowed to stir for 30 minutes at 4$^{O}$C. After stirring with heme solution the pellet was sonicated in a Fisher Scientific FS20 sonicator for 30 minutes. After sonication the pellet solution was centrifuged for 25 minutes at 26,892 X g (15000 RPM, KA-21.5 rotor with 50 ml centrifuge tubes). The supernatant was collected and 0.01 ml of heme solution per gram of original cell pellet (10 mg heme/ ml of 0.1 M NaOH) was added. The supernatant was allowed to stir at 4$^{O}$C for 1 hr. After stirring, the supernatant was centrifuged for 15 minutes at 26,892 X g (15000 RPM, KA-21.5 rotor with 50 ml centrifuge tubes). The supernatant and the supernatant from the earlier step were combined and dialyzed in lysis buffer. After dialysis, the DHP solution was centrifuged for 15 minutes at 26,892 X g (15000 RPM, KA-21.5 rotor with 50 ml centrifuge tubes). The supernatant was collected and the pH was determined.

DHP was purified using CM52 cation exchange resin (Whatman Cat. #4057050) in a Kontes* Brand Flex-Column* Economy, K4204000-1050. Approximately 80 ml of resin

was equilibrated with 3.5L of column buffer (20 mM Phosphate pH 5.0). The protein solution was loaded onto the equilibrated column and was washed with 80 ml of column buffer. A 300 ml linear gradient of 20 mM Phosphate pH 5.0 to 20 mM Phosphate 0.5 M NaCl, pH 5.0 was used to elute the protein. Fractions were collected and analyzed for DHP using a UV-Vis spectrophotometer. All fractions with a purity number of 2.5 or better were pooled. The pooled fractions were concentrated by Amicon centriprep YM-10 (cat. # 4321). The concentrated protein solution was then loaded onto an 80 ml sephacryl S-300 (Fluka cat. # G01051) Kontes* Brand Flex-Column* Economy, K4204000-1050 column in 20 mM Phosphate pH 5.0 buffer. Fractions from this column were analyzed by SDS-Page.

The addition of hemin to the protein to constitute apo-dehaloperoxidase (*vide supra*) resulted mixed oxidation states of the heme. In order to ensure that only the ferric form was isolated, the DHP protein was treated with 1.7 molar excess potassium ferricyanide (Fisher P232). Excess ferricyanide was removed by size exclusion chromatograpy carried out by using a sephedex G-25 column. The protein was concentrated using an Amicon centriprep YM-10 (4321) and the purity of the DHP was determined from a ratio of the absorbances at 409 and 280 nm. Purity numbers ($A_{280}/A_{409}$) in this case were always greater than 3.4. The concentration of the DHP was determined spectrophotometrically at 409 nm using a molar absorptivity of $1.88 \times 10^5$ $M^{-1}$ $cm^{-1}$.

**2.3 Results and Discussion**

Polymerase chain reaction amplification of dehaloperoxidase gene with and without additional codons for an N-terminus His tag was successful. Figure 2.1 is a 1% agarose gel showing a MW ladder in the far right lane, the next three lanes show the successful PCR amplification of 6x His DHP resulting in an N-terminus tag, lanes 5-7 show no bands, which

means the attempt to make a C-terminus His tag was not successful. The last lane of the gel in figure 2.1 shows a successful amplification of the gene for the non his tagged DHP gene.

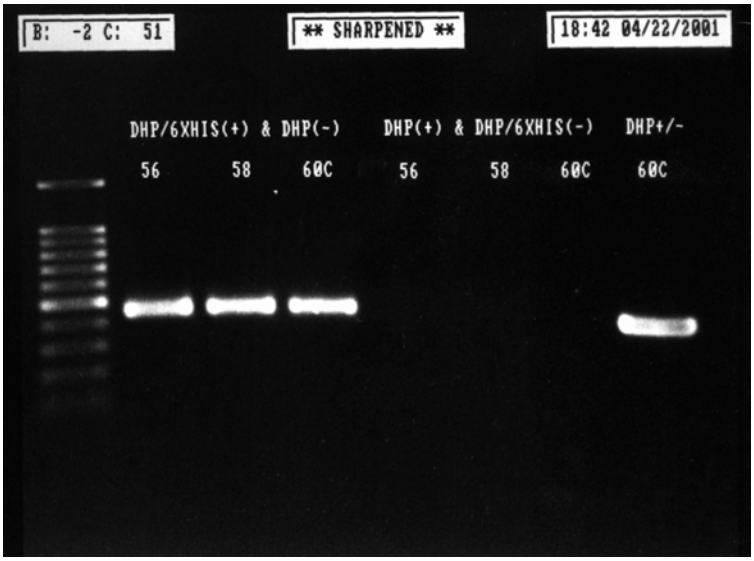


Figure 2.1 1% Agarose gel lane 1 at far right contains MW marker, lanes 2-4 contain gene for the N-terminus His tagged gene, lanes 5-7 are blank, lane 8 contains the non his tagged gene.

Protein expression in Rosetta (DE3) pLys cells resulted in ~ 10 mg of His and non His tagged protein for every 50g of cell pellet. Expression of the same plasmids in BL-21 (DE3) pLys cells did not result in any measurable amounts of protein. The result is attributed to the AGG codon. Figure 2.2 shows the sequence of the DHP gene with the AGG codons that *E. coli* does not read are highlighted in yellow. An initial inspection of the codons present in the DHP gene sequence compared with the known codons used in *E.coli* was done. This led to the determination that the AGG codon for the amino acid arginine, was not used by *E. coli*.

atg ggg ttt aaa caa gat att gcc acc atc cgc ggt gat ctc agg acc tat gca

cag gac att ttc ctc gca ttt ttg aat aag tac ccg gac gag agg agg tac ttc

aaa aac tat gtc ggc aaa tct gac caa gag ctc aag tca atg gcc aag ttc ggt

gat cac act gag aaa gtg ttc aac ctg atg atg gaa gtt gcg gac cga gcc acc

gat tgt gtc ccc ctt gcg tcc gac gcc aac aca ctc gtc cag atg aaa cag cat

tcc agc ctg acg act gga aac ttc gag aaa ctg ttc gtg gca ttg gtg gag tat

atg aga gcg tct ggc cag tcc ttc gac tct caa agc tgg gat agg ttc ggc aag

aat ttg gtc tcc gcg ctg agc agc gca ggc atg aag tag

Figure 2.2. Sequence of dehaloperoxidase with AGG codons highlighted. *E. coli* does not naturally read the AGG codon.

Dehaloperoxidase and 6xHis tagged Dehaloperoxidase have been successfully cloned and expressed in *E. coli*. The use of the Rosetta cell line proved to be the key to overcoming the codon preferencing problem, which was not allowing protein to be produced in other cell lines. Protein purification procedures for both forms of DHP have been developed. With current methods we are now able to produce the quantity and quality of protein necessary for further experiments.

## References

9. LaCount, MW., Zang, EL., Chen, YP., *et al*. The crystal structure and amino acid sequence of dehaloperoxidase form *Amphitrite ornata,* indicate common ancestry with globins, Journal of Biological Chemisty 2000; 275: 18712 – 18716.
10. Zhang, E., Chen, YP., Roaach, MP., *et al*. Crystallization and initial spectroscopic characterization of the heme-containing dehaloperoxidase from the marine polychaete *Amphitrite ornata,*. Acta Cryst. 1996; **D52**: 1191-1193**.**
11. Roach, MP., Chen, YP., Dawson, JH., *et al*. *Notomastus lobatus* Chloroperoxidase and *Amphitrite ornata,* Dehaloperoxidase both contain histidine as their proximal heme iron ligands, Biochemistry 1997; **36**: 2197-2202.
12. Lebioda, L., LaCount, MW., Woodin, SA., *et al* An enzymatic globin from a marine worm Nature 1999; **401**: 445
13. Chen, YP., Woodin, SA., Lincoln, DE., and Lovell, CR., An unusual dehalogenating peroxidase from the marine terebellid polychaete *Amphitrite ornata,* The Journal of Biological Chemistry 1996; **9**: 4609-4612.
14. Han, K., Woodin, SA., Ely, B., *et al*. *Amphitrite ornata,* a Marine Worm, Contains Two Dehaloperoxidase Genes, Marine Biotechnology 2001; **3**: 287-292
15. Proteomics, *Tools for Protein Expression, Purification, & Analysis* » Protein Expression Hosts, Bacterial Rosetta™ 2000. Novagen product information manual accompanying product catalog number 70956-3.

# Chapter 3: Assays of Dehaloperoxidase Enzyme Activity

### 3.1 Introduction

Dehaloperoxidase has been reported to have peroxidase activity. X-ray crystal structures have shown that DHP has a globin fold and a distal valine. Both the globin fold and distal valine disputes the reported peroxidase activity. Peroxidases and globins typically have a distal histidine residue not a valine. The distal histidine residue plays a key role in peroxidase activity and DHP was the first globin reported to have peroxidase activity. Dehaloperoxidase lies in a unique junction in the study of structure-function relationship due the unusual characteristics of a globin fold coupled with peroxidase activity.

The enzyme Horseradish Peroxidase (HRP, EC 1.11.17) is a highly studied peroxidase that is commercially available; thus, we chose to model DHP assays after the current assays in use for HRP[1,2]. Several assays were developed to characterize the peroxidase activity of DHP, and a modified standard peroxidase assay was utilized as well. Since a viable sample of the native enzyme from the marine worm *Amphitrite ornata* was not obtained, no direct comparison to recombinant forms was made.

Horseradish peroxidase is a very different enzyme than dehaloperoxidase. For instance, HRP is a plant enzyme that has native glycosylations, a calcium ion required for function, disulfide bonds, and a channel that allows the substrate to approach the heme active site[1,2]. Dehaloperoxidase is a marine worm enzyme that has no glycosylations, no required calcium ions or disulfide bonds, and has a true binding pocket for substrate[3,4]. The differences include the amino acid residues in the distal pocket, HRP has a distal histidine where, DHP has a distal valine[3-5].

The difference between HRP and DHP extended into their expression as recombinant proteins. The production of HRP in *E. coli* resulted in the protein being expressed in

inclusion bodies and once the protein was freed from the inclusion bodies, the HRP protein required folding since the *E. coli* produced HRP did not fold with proper disulfide bond formations[1]. Dehaloperoxidase was not expressed in inclusion bodies. Despite the many differences between dehaloperoxidase and HRP, we were able to compare reaction rates using UV – Vis and stopped – flow analysis.

Peroxidase enzymology is complicated due to the formation of an irreversible enzyme substrate complex, and two-substrate two-product reactions. It is common for peroxidases to have irreversible reactions along with detectable covalent compounds as intermediates, compound I and II, instead of enzyme-substrate complexes[1]. The Michaelis-Menton approach to enzymology does not apply to the study of peroxidases. The Michaelis-Menton approach is based on the concept that the enzyme-substrate interaction is reversible and not stable enough to be a long lived species.

A typical peroxidase reaction is presented with the two-substrate two-product reaction scheme in Figure 3.1. Native protein is activated to the compound I state by peroxide. Next, one substrate molecule interacts with compound I and product one is released, which then modifies the enzyme to the compound II form. The compound II form of the enzyme reacted with a second substrate, which was then followed by the release of product two and the regeneration of the native protein see Figure 3.1. Alternatively the protein in the Oxy state of the protein can react with an electron to generate the Peroxy form of the protein. The Peroxy form can react with two $H^+$ to generate compound I. Equations 3.1 – 3.4 make up the currently accepted mechanism for peroxidase cycle, where AH represented a reducing substrate and $^{\cdot}A$ was the resulting free radical[1].

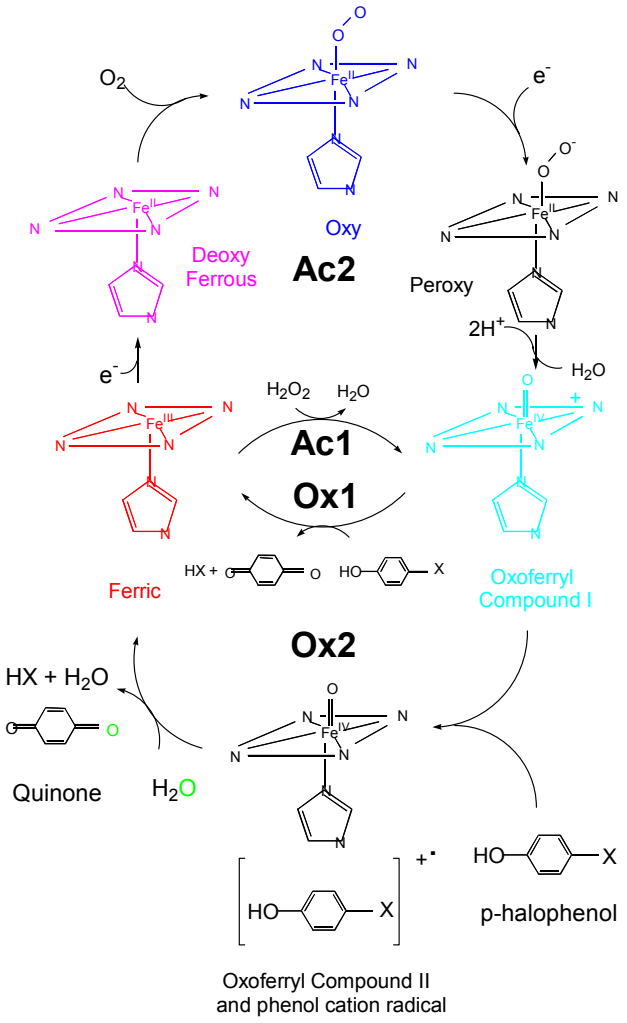


Figure 3.1. is a description of a peroxidase and monooxygenase pathways for oxidative dehalogenation of p-halophenols. The X label represents F, Cl, or Br. The pathways Ac1 and Ac2 are two possible oxygen activation pathways involving peroxide and oxygen binding (with electron transfer), respectively. The two possible oxidation mechanisms involve oxygen atom transfer (Ox1) and oxidation via electron transfer in two steps (Ox2). The oxygen of the quinone product is derived from solvent water in Ox2 as indicated by the green color of the O atom.

Native peroxidase + $H_2O_2 \xrightarrow{k_1}$ compound I + $H_2O$ (eq. 3.1)

Compound I + AH $\xrightarrow{k_2}$ compound II + $\cdot$A (eq. 3.2)

Compound II + AH $\xrightarrow{k_3}$ Native peroxidase + $\cdot$A + $H_2O$ (eq. 3.3)

---

$H_2O_2 + 2AH \rightarrow 2H_2O + 2.A$ (eq 3.4)

Notice the 1:2 stoichiometry between $H_2O_2$ and substrate. The rate of substrate consumption was twice that of $H_2O_2$. Equation 3.5 was the equation that represented the rate of a peroxidase cycle[1,6]. Figure 3.2 was a pictorial representation of a peroxidase cycle as a ping pong mechanism[1]. The one electron product is represented as ·A. ·A is produced when the product can diffuse out of the active site faster than the electron transfer rate for two electrons. Although we cannot say for sure, we do not believe that this is the mechanism of DHP. We believe that diffusion of substrate into and out of DHP is slow enough to allow for a two electron product to be formed.

$\upsilon/[E]_o = ( 1/k_1[H_2O_2])^{-1} + (k_2 + k_3/ k_2 k_3[AH]$ (eq. 3.5)

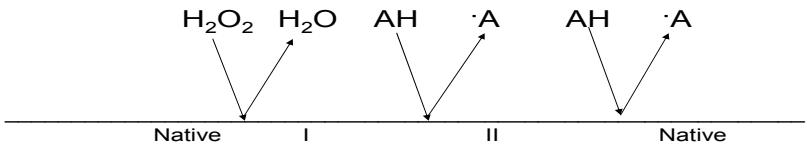


Figure 3.2 shows a peroxidase cycle depicted in a ping-pong as mechanism. Complexes between substrates and enzyme were short lived and nearly impossible to detect. The product is shown to leave as fast as substrate can interact with enzyme. Compound I is represented by I and compound II is represented by II.

A mechanism that is used to depict the formation of compound I of heme peroxidases is the Poulos-Kraut push/pull mechanism. In this mechanism the push rises from the partially negatively charged or polarized histidine ligand to the heme iron. The increased basicity of the axial ligand stabilizes higher oxidation states (e.g. Fe(IV)) so that compounds I and II can be formed. In peroxidases, the residues that play a role in the push are Asp and His, along with the iron of the heme. An analogy has been made between this triad and the catalytic triad of serine proteases[7]. In serine proteases the catalytic triad Asp-His-Ser increase the basicity (nucleophilicity) of the serine residue for attack on the carbonyl carbon of the peptide bond. The pull in the push/pull mechanism is comprised of interactions of amino acids in the distal pocket with bound peroxide to facilitate oxygen-oxygen bound cleavage in peroxide. This in turn is required for the formation of compound I. Since dehaloperoxidase had a distal valine, not a histidine, a modified pull step was proposed by our group. The proposed mechanism does not have a direct abstraction of a proton by the distal histidine residue as does the Poulos-Kraut mechanism.

**3.2 UV-Vis Spectroscopic Assays**

Using a UV-Vis spectrophotometer to monitor reactions catalyzed by DHP and 6x His DHP, the disappearance of substrate and the appearance of product were observed. It was also possible to observe the destruction of both recombinant forms of DHP by peroxide. All UV-Vis spectroscopic assays were performed on a Hewlett Packard chemstation UV-Vis spectrophotometer, using a Hewlett Packard 89090A, temperature controlled cell holder. All assays of DHP were done with the same stock of protein that was done for the 6x His DHP. For comparison purposes, assays of DHP and 6x His DHP were performed with the same stock solutions of substrate and buffer.

### *3.2.1 DHP and 6x His DHP assays using 2,4,6-Trifloropehenol, 2,4,6-Trichlorophenol, 2,4,6-Tribromophenol, and 2.4.6-Triiodiophenol*

In all assays, both recombinant forms of dehaloperoxidase were assayed at 25 $^{o}$C, while being stirred at 250 rpm in 20 mM potassium phosphate pH 6.0 buffer, 156 μM 2,4,6-trihalophenol, 50 μM hydrogen peroxide and 0.5 μM DHP. The reaction was initiated with the addition of hydrogen peroxide. UV- Vis spectra was collected every 5 seconds for 100 seconds which resulted in 20 spectra. Stock solutions of the trihalophenols were made by weighing out solid and dissolving the solid into 20 mM potassium phosphate pH 6.0. Heat from a hot plate was necessary to dissolve the 2,4,6-trichlorphenol, 2,4,6-tribromophenol, and the 2,4,6-triiodiophenol in water. The 2,4,6-triflorophenol did not require heating, since it dissolved in aqueous solution, but it must be mixed well because it had a tendency to stick to walls of the container. All substrate solutions were made freshly prior to use and discarded when the UV – Vis spectrum of the solution began to differ from its original spectra. Solutions were usually stable for four to six hours after being made. All halophenols were ordered from Acros Organics at 98% purity or better and were used without further purification. Buffer components and hydrogen peroxide were purchased from Fisher Scientific Inc. Co. and used without further purification.

### 3.2.2 Hydrogen Peroxide Susceptibility

Peroxidases were activated when a peroxide molecule was available to initiate a reaction between the peroxidase and substrate. Since peroxide has a vital role in the reactions of peroxidases, the tolerance of dehaloperoxidase to peroxide became a central issue. The peroxide susceptibility study was addressed when standard HRP assays caused dehaloperoxidase to degrade. The heme degradation was noticed when UV – Vis

spectroscopic assays exhibited a dramatic decrease in the Soret band of dehaloperoxidase, but there was very little change in the Soret band of HRP.

Since dehaloperoxidase has a globin fold and peroxidase activity, its response to peroxide is of great interest. In the hydrogen peroxide susceptibility studies we chose to use HRP as a model peroxide and horse heart myoglobin (HHMb) as a typical globin. Several hydrogen peroxide susceptibility assays were required to determine whether dehaloperoxidase responds to peroxide as a peroxidase or as a globin. In other words, are compounds I and II formed and does the protein show stability with respect to degradation by peroxide.

Hydrogen peroxide susceptibility was determined using UV-Vis spectroscopy. Protein was added to a 1cm cuvette that had been blanked using 10 mM potassium phosphate pH 7.0. Hydrogen peroxide was added to the cuvette at 1 to 1000 molar ratio of protein to peroxide. The reaction was monitored every 3 to 5 seconds after addition of peroxide. Hydrogen peroxide susceptibility of HHMb was determined at a 1 to 100 molar ratio of protein to peroxide, due to its rapid degradation at the higher ratio.

**3.3 Stopped – Flow Assays of 6x His DHP**

Stopped-flow analysis of HRP, is a common technique which is employed to obtain rate constants in work done in the laboratory of H. Brian Dunford[2]. We chose to use 2,4,6-tribromophenol in the stopped-flow assays, since it represented a substrate which is active for both recombinant dehaloperoxidase and HRP. We wish to thank Dr. Clay Clark of Department of Biochemistry at North Carolina State University, and members of his laboratory for the opportunity to use their Applied Photohpysics SX.18MV Stopped-flow Reaction Analyzer.

For the stopped-flow experiments one drive syringe contained the 2,4,6-tribromophenol, 20 mM potassium phosphate pH 6.0, 1.1μM or 11μM hydrogen peroxide and 0.1M potassium nitrate while the second drive syringe contained the 6x His DHP or HRP at a concentration of 1.2μM or 12μM and 0.1M potassium nitrate. Solutions of 2,4,6-tribromophenol were monitored via UV-Vis, and once the UV-Vis spectrum of the 2,4,6-tribromophenol solution began to vary from its original spectrum, it was discarded and a new solution was made. Solutions of 2,4,6-tribromophenol were typically stable for six hours.

Drive and storage syringes were rinsed extensively with 18MΩ water, followed by flushes with buffer solutions and reaction solution before use and between kinetic runs. The stopped-flow apparatus was cleaned using 10 shots of 18 ΩM, water (a shot was one mixing reaction) followed by 10 shots of buffer solution, followed by 10 shots of the reaction solution. Once the appropriate solutions had been shot, an overlay of shots 9 and 10 were done to see if there were variations. If there were no variations between shots 9 and 10 then the experiment was ready, but if there were variations further cleaning was necessary.

Shot volume was set to 500μL for experiments with 1.2μM 6x His DHP or HRP and 1.1μM hydrogen peroxide and the volume was decreased to 120μL for 12μM 6x His DHP or HRP and 11μM hydrogen peroxide. The larger volume for the more dilute experiment was necessary to obtain data with less noise. Since the more concentrated experiment allowed us to use a smaller volume, we were able to collect data at constant pressure conditions. The constant pressure condition eliminated much of the noise that plagued the lower concentration/higher volume experiment. All future stopped-flow experiments should be done at the higher concentration/lower volume conditions.

**3.4 UV-vis Spectroscopic Assays Results of DHP and 6x His DHP assays using 2,4,6-Trifloropehenol, 2,4,6-Trichlorophenol, 2,4,6-Tribromophenol, and 2.4.6-Triodiophenol**

Since the native substrate for DHP is 2,4,6-tribromophenol, UV-vis absorption assay was developed for this substrate and was then applied to other substrates. To identify the differences in the two forms, our initial goal was to assay the recombinant DHP and the recombinant His tagged DHP. In Figure 3.3 DHP was assayed with 2,4,6-tribromophenol as the substrate. The initial spectrum was black, which was taken before the addition of peroxide. Each spectrum after the initial black spectrum was taken approximately five seconds apart. The color scheme following our initial black reading follows this pattern: orange, yellow, green, blue, and then purple. The last spectrum was taken 97 seconds after the initiations of the reaction.

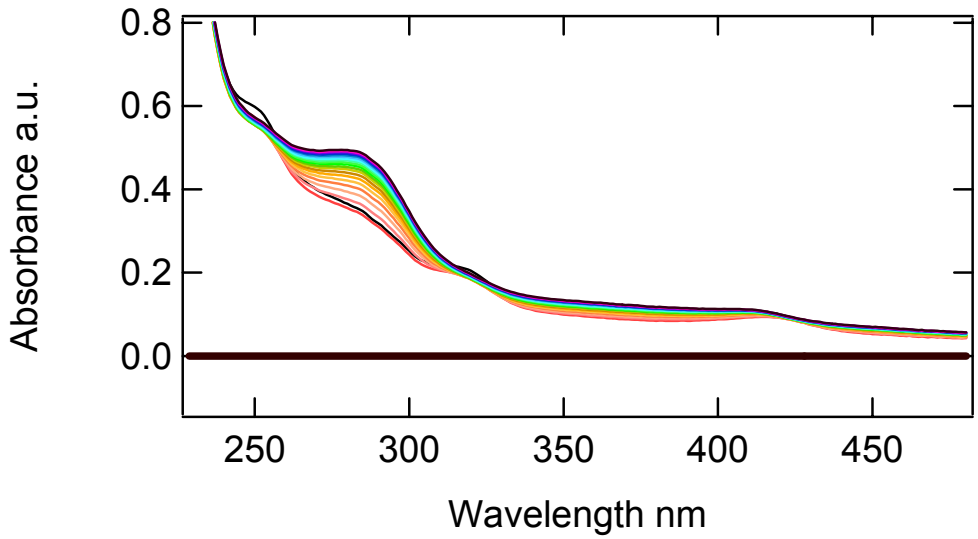


Figure 3.3 UV-Vis assay of DHP, 2,4,6-tribromophenol at pH 6.0.

The difference spectrum in Figure 3.4, of the first and last spectra showed the wavelengths of the greatest interest to be 289 nm, 320nm, and 420nm. The peak at 289nm was attributed to the formation of product; while, the dip at 320 nm represented the consumption of the substrate. The valley formed at 420 nm was due to the heme shift and the eventual degradation of the protein (please see section 3.5 on peroxide susceptibility for an explanation of this).

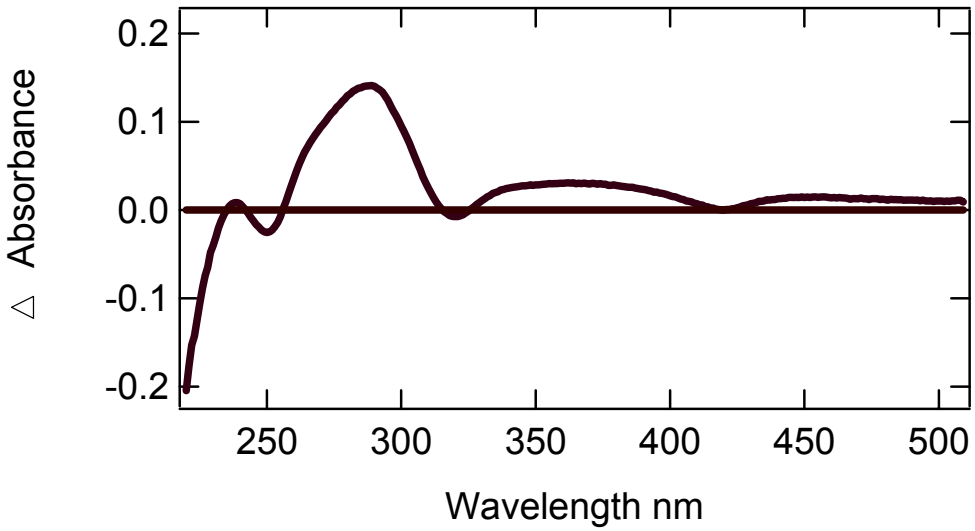


Figure 3.4 Difference spectrum of the first and last spectra collected from a UV-Vis assay of DHP in 20 mM potassium phosphate pH 6.0 using 2,4,6-tribromophenol as the substrate.

In assays of 6x His, DHP showed identical results (see Figure 3.5). The difference spectrum in Figure 3.4 of the first and last spectra showed the wavelengths of the greatest interest to be 289 nm, 320nm, and 407nm. The peak at 289nm and 320 nm represented the substrate and product as it was in the assay of DHP. Note that in the assays of DHP, the wavelength that represented the difference in the heme was 420nm. The valley formed at 407 nm was due to the heme shift and eventual degradation of the protein.

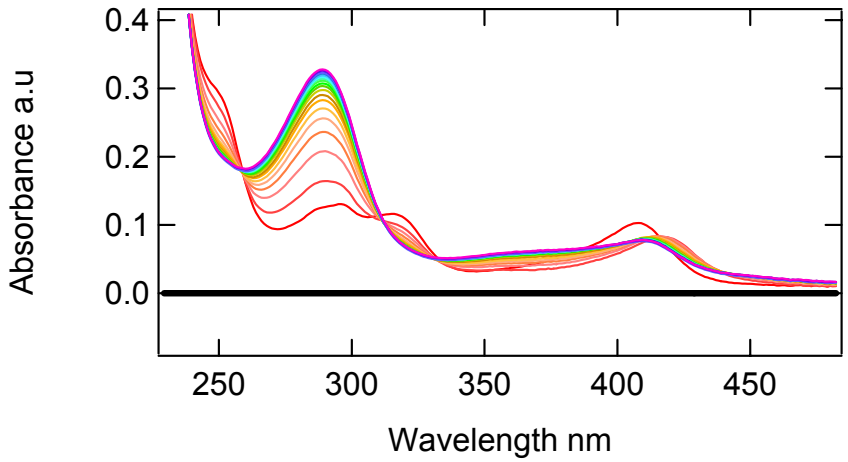


Figure 3.5 UV-Vis assay of 6x His DHP, 2,4,6-tribromophenol at pH 6.0.

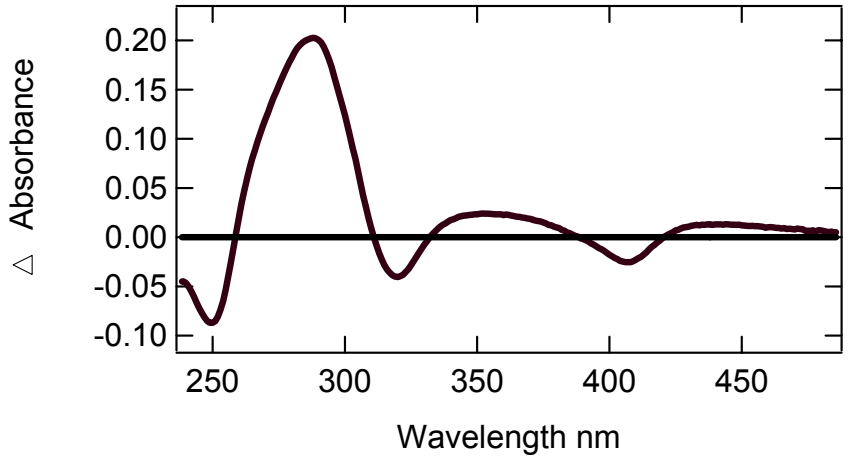


Figure 3.6 Difference spectrum of the first and last spectra collected from a UV-Vis assay of 6x His DHP in 20 mM potassium phosphate pH 6.0 using 2,4,6-tribromophenol as the substrate.

The assays of DHP and 2,4,6-triflorophenol, 2,4,6-trichlorophenol, and 2,4,6-triiodiophenol showed similar results, with the major difference being in the wavelengths representing the substrate consumption and the yield of product. In comparing the result of the difference assays for the two forms of dehaloperoxidase, we obtained similar peaks for substrate and products. The major variation to this was that the heme shift appeared different between 6x His DHP and DHP. See figures 3.7 – 3.18 and table 3.1.

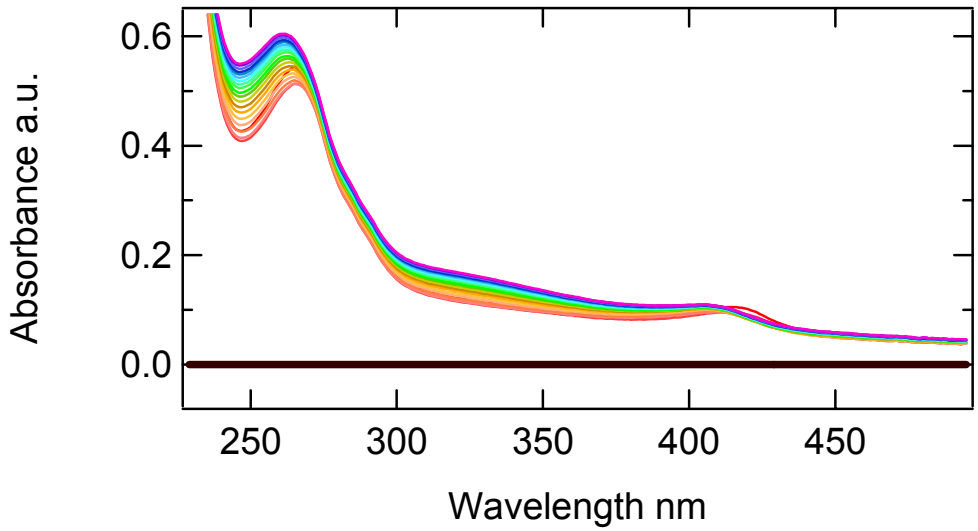


Figure 3.7 UV-Vis assay of DHP, 2,4,6-triflorophenol at pH 6.0.

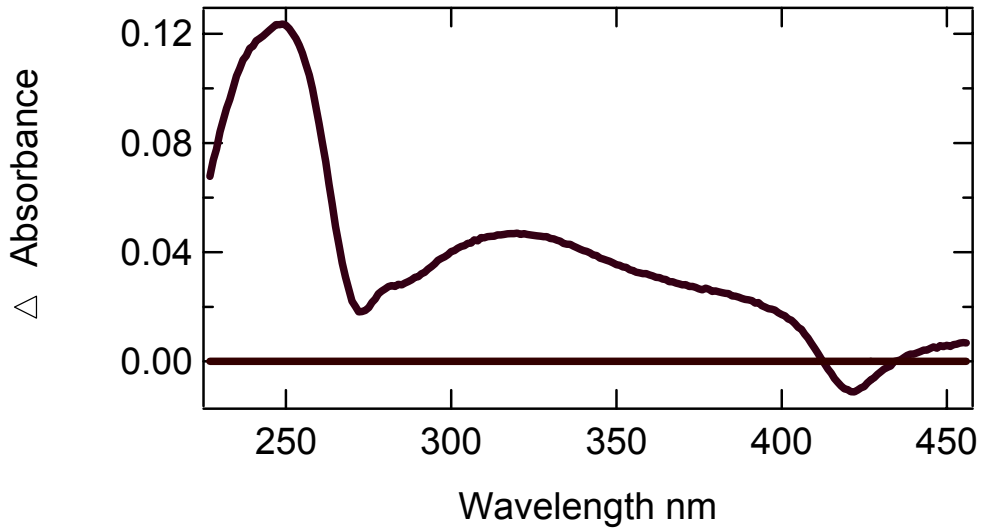


Figure 3.8 Difference spectrum of the first and last spectra collected from a UV-Vis assay of DHP in 20 mM potassium phosphate pH 6.0 using 2,4,6-triflorophenol as the substrate.

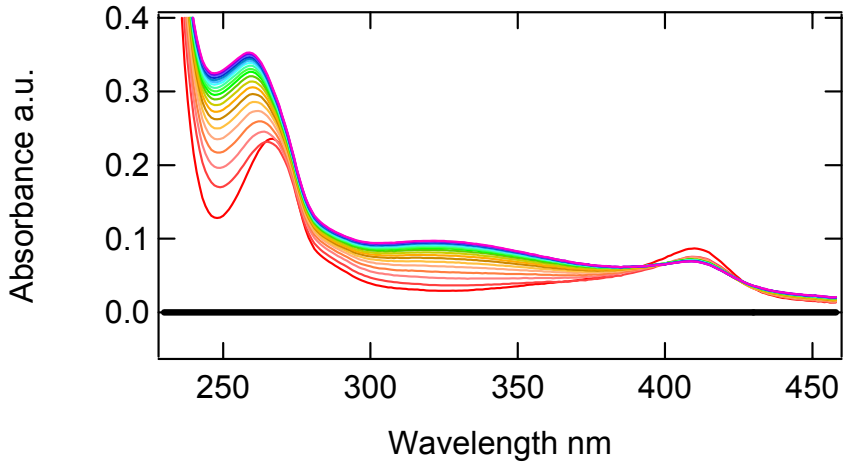


Figure 3.9 UV-Vis assay of 6x His DHP, 2,4,6-triflorophenol at pH 6.0

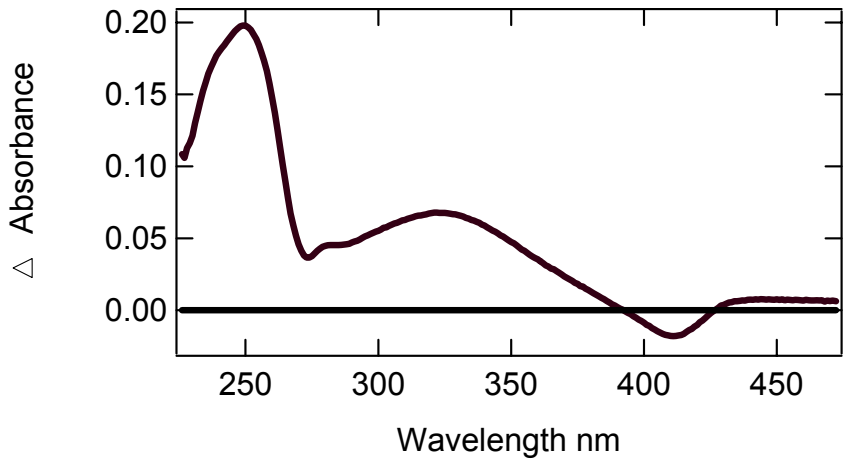


Figure 3.10 Difference spectrum of the first and last spectra collected from a UV-Vis assay of 6x His DHP in 20 mM potassium phosphate pH 6.0 using 2,4,6-triflorophenol as the substrate.

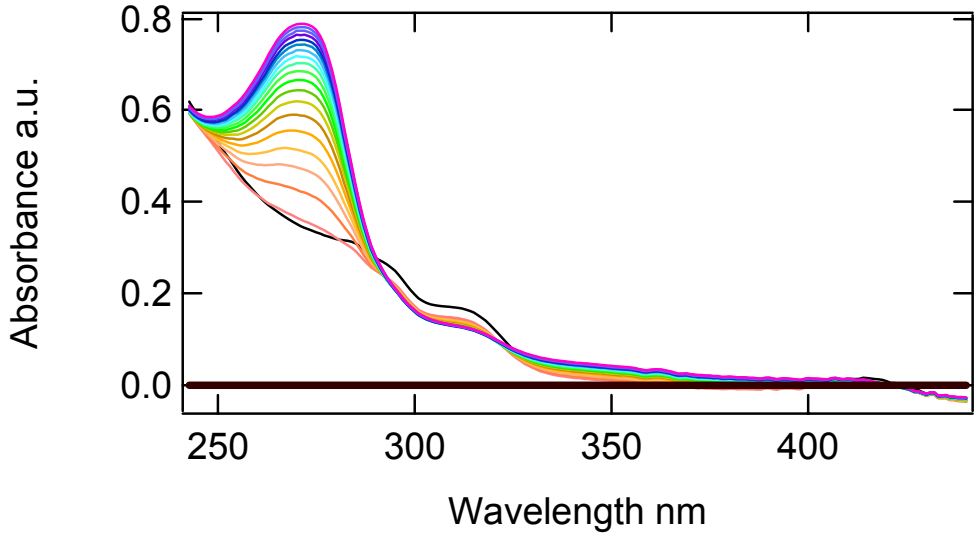


Figure 3.11 UV-Vis assay of DHP, 2,4,6-trichlorophenol at pH 6.0

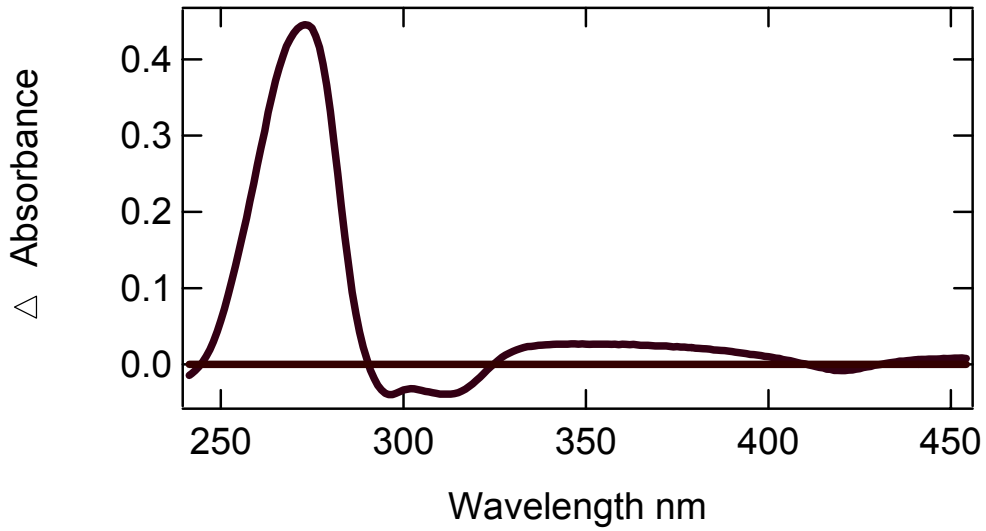


Figure 3.12 Difference spectrum of the first and last spectra collected from a UV-Vis assay of DHP in 20 mM potassium phosphate pH 6.0 using 2,4,6-trichlorophenol as the substrate.

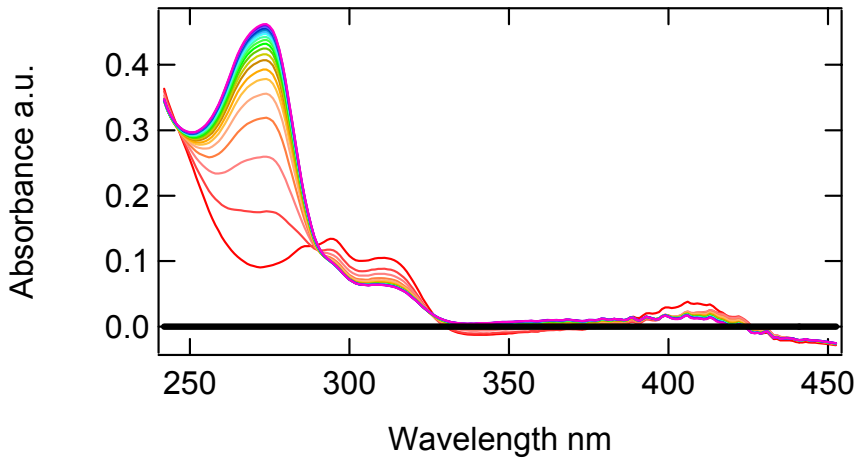


Figure 3.13 UV-Vis assay of 6x His DHP, 2,4,6-trichlorophenol at pH 6.0

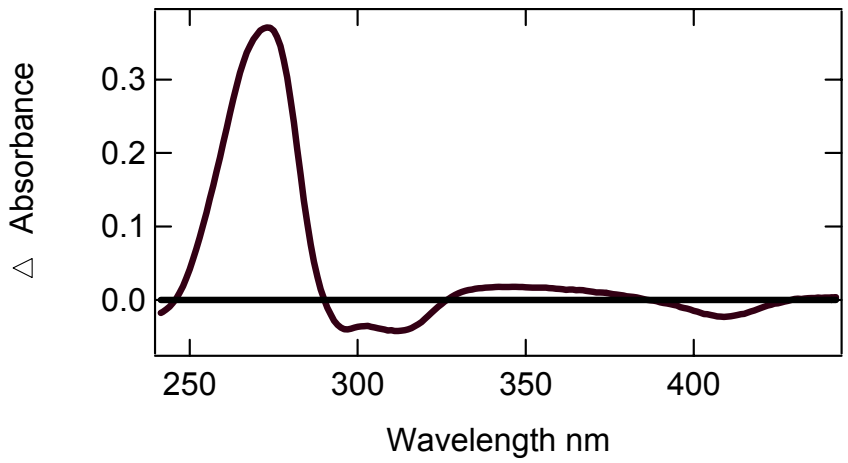


Figure 3.14 Difference spectrum of the first and last spectra collected from a UV-Vis assay of 6x His DHP in 20 mM potassium phosphate pH 6.0 using 2,4,6-trichlorophenol as the substrate.

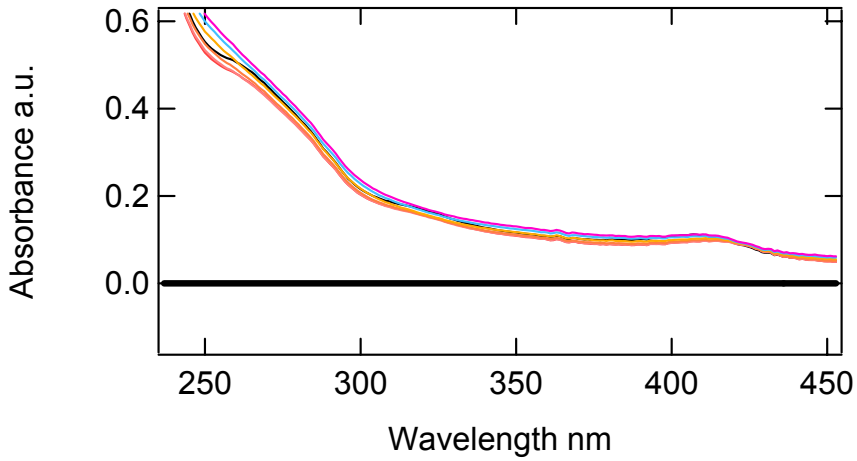


Figure 3.15 UV-Vis assay of DHP, 2,4,6-triiodiophenol at pH 6.0.

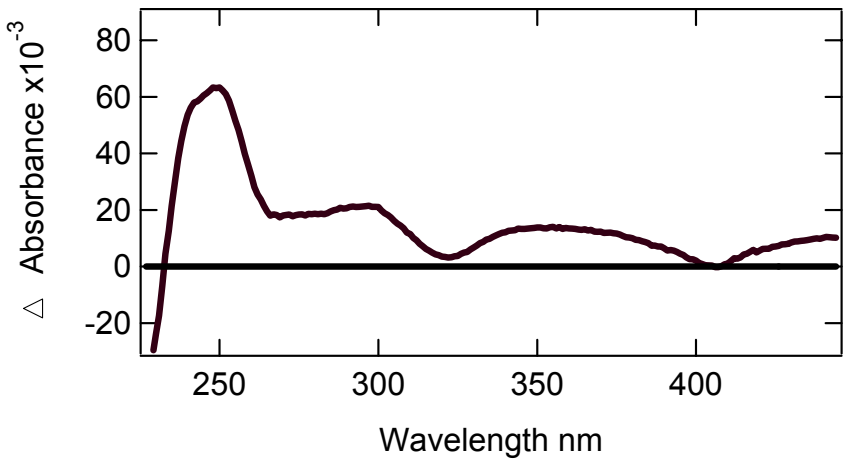


Figure 3.16 Difference spectrum of the first and last spectra collected from a UV-Vis assay of DHP in 20 mM potassium phosphate pH 6.0 using 2,4,6-triiodophenol as the substrate.

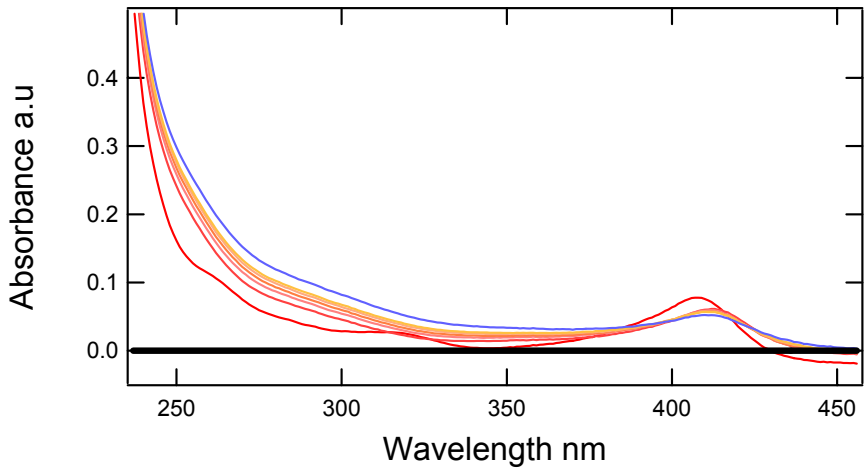


Figure 3.17 UV-Vis assay of 6x His DHP, 2,4,6-triiodiophenol at pH 6.0

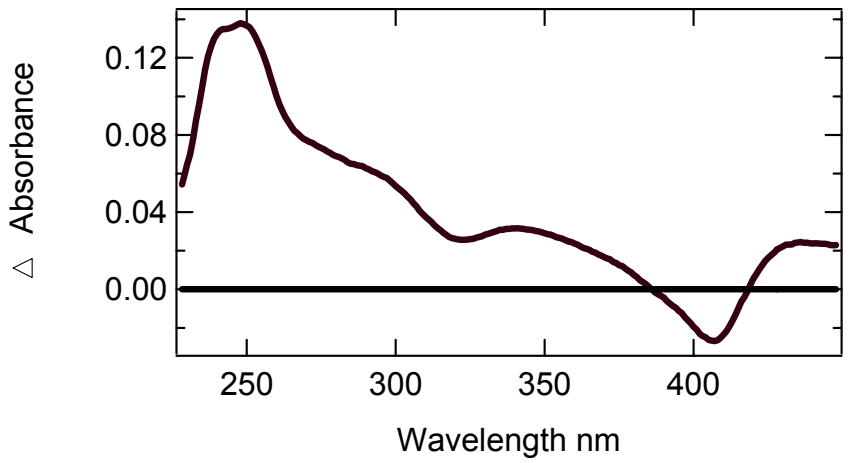


Figure 3.18 Difference spectrum of the first and last spectra collected from a UV-Vis assay of 6x His DHP in 20 mM potassium phosphate pH 6.0 using 2,4,6-triiodophenol as the substrate.

| Substrate | Protein | Product λ (nm) | Substrate λ (nm) | Heme shift λ (nm) |
|---|---|---|---|---|
| 2,4,6-tribromophenol | DHP | 289 | 320 | 420 |
| | 6x His DHP | 289 | 320 | 407 |
| 2,4,6-trichlorophenol | DHP | 272 | 312 | 420 |
| | 6x His DHP | 272 | 312 | 409 |
| 2,4,6-triiodiophenol | DHP | 248 | 323 | 406 |
| | 6x His DHP | 248 | 323 | 407 |
| 2,4,6-triflorophenol | DHP | 273 | | 421 |
| | 6x His DHP | 273 | | 411 |

Table 3.1 Table of wavelength for products, substrate and heme shifts for reactions with DHP and 6x His DHP.

6x His Dehaloperoxidase can use floro-, chloro-, bromo- and iodio- trihalogenated phenols as substrates. We have shown that assays of 6x His DHP with trihalogenated phenols results in substrate consumption and heme degration. Limited product turnover is attributed to heme degration. Definitive rates of product formation and substrate consumption can not be calculated from the UV – vis assays do the heme degration.

**3.5 Hydrogen Peroxide Susceptibility Results**

Since dehaloperoxidase has a globin fold and peroxidase activity its response to peroxide is of great interest. Assays that use a molar ratio of 1:1 of protein to peroxide would have theoretically generated compound I. In all of the assays shown thus far, an excess of peroxide was used. The use of excess peroxide results in the formation of compound II in all of the reactions of 6x His DHP and HRP. A Soret band at 420 nm, which was a typical value of a compound II Soret, was detected using the UV-vis absorbance assay.

In Figure 3.19, 6x His DHP has an initial absorbance at 420 nm, which resulted from 0.07 μM of protein (red trace). Five seconds after the addition of hydrogen peroxide (final concentration of 70 μM) was added to the protein solution, the Soret shifted to 420 nm which was indicative of compound II (yellow trace). One hundred and one seconds after the addition of peroxide, the Soret shifted back to the original location, but the intensity was decreased (blue trace). At 101 seconds the absorbance of the Soret represented 0.03 μM of 6x His DHP present. Addition of peroxide to 6x His DHP resulted in rate $5.7 \times 10^{-6}$ μM of 6x His DHP degraded per second per μM of peroxide.

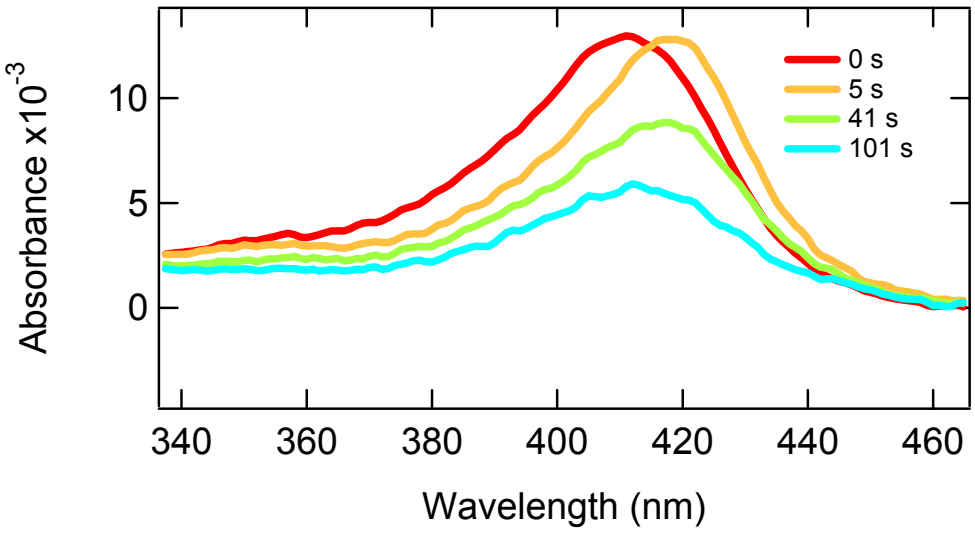


Figure 3.19 Hydrogen Peroxide susceptibility test on 6x His DHP to probe tolerance to excess peroxide.

The red trace represented 6x His DHP before the addition of peroxide in the resting state; note, the Soret maximum is at 414 nm. The orange trace which was taken 5 seconds after the addition of peroxide and showed a shift in the Soret maximum to 420 nm, which is typical of compound II. The green trace was a mixture of resting 6x His DHP and compound II; note, it was broader and had a Soret maximum at 418 nm. At 101 seconds after the addition of peroxide the Soret maximum was back to 414 nm, though the intensity was lower (blue trace).

Since the Soret was shifting, we chose to look at the area under the Soret band instead of a single wavelength for an indicator of how much intact 6x His DHP was present at the times indicated in the figure above. We chose to define the Soret band from 340 nm to 460 nm. When we calculated the area under the Soret band between 340 nm and 460 nm and graphed the area vs. time, we obtained Figure 3.20. In this figure the degradation of 6x His

DHP was exponential. An exponential decay was expected for a pseudo first order decay and since an excess of peroxide induces a pseudo first order reaction, this result was expected.

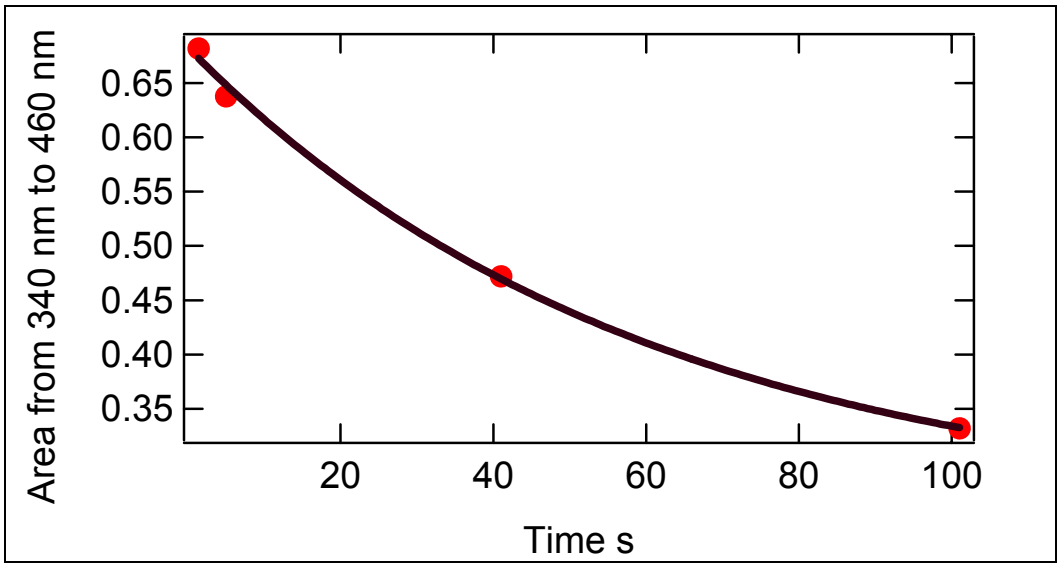


Figure 3.20 Graph of the area between 340 nm and 460 nm that lies under the Soret band for 6x His DHP vs. seconds after addition of 1000 molar excess of peroxide was added to the protein solution.

Hydrogen peroxide susceptibility tests of HRP showed a very different response to excess peroxide. In Figure 3.21 the red trace represented HRP before peroxide was added. Notice that the Soret maximum was at 420 nm; thus, compound II was present. According to Dr. H Brian Dunford this was common when there are impurities in the water used to dissolve the freeze dried protein. The resting state of HRP was 403 nm; thus, we are seeing compound II at the onset of the experiment. Thirty-five seconds after the addition of 1000 molar excess peroxide we saw that the Soret band had decreased very slightly (green trace). Eighty-three seconds after the addition of peroxide we noticed a decrease in the Soret band,

but no further decrease was noted (blue trace). The decay of HRP do to the addition of peroxide is negligible during the time of this experiment.

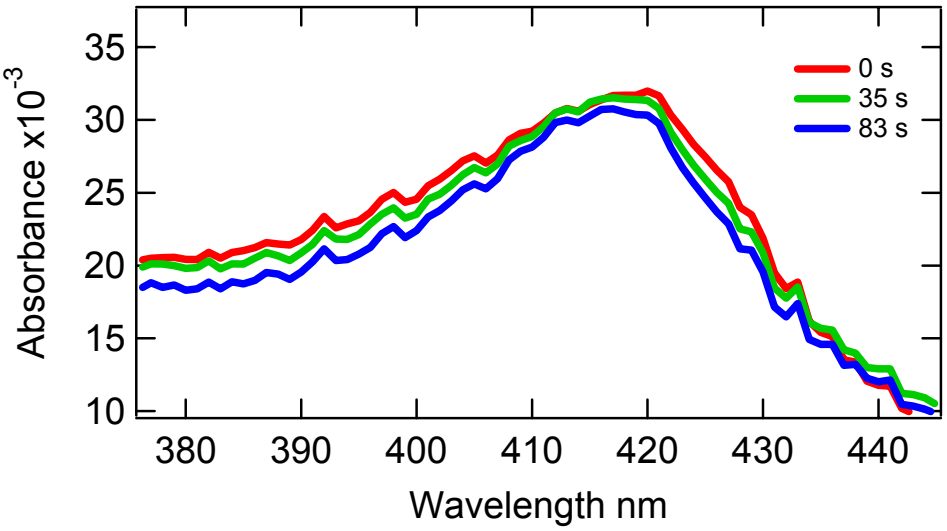


Figure 3.21. Assay of hydrogen peroxide susceptibility test on HRP to probe HRP's tolerance to excess peroxide.

Since the Soret was shifting in the 6x His DHP assay we chose to look at the area under the Soret band instead of a single wavelength for an indicator of how much intact 6x His DHP was present at different times. We chose to do the same area calculation with the HRP data. We chose to define the Soret band from 380 nm to 440 nm. When we calculated the area under the Soret band between 380 nm and 440 nm and graphed area vs. time, we obtained Figure 3.22. In this figure the degradation of HRP is exponential.

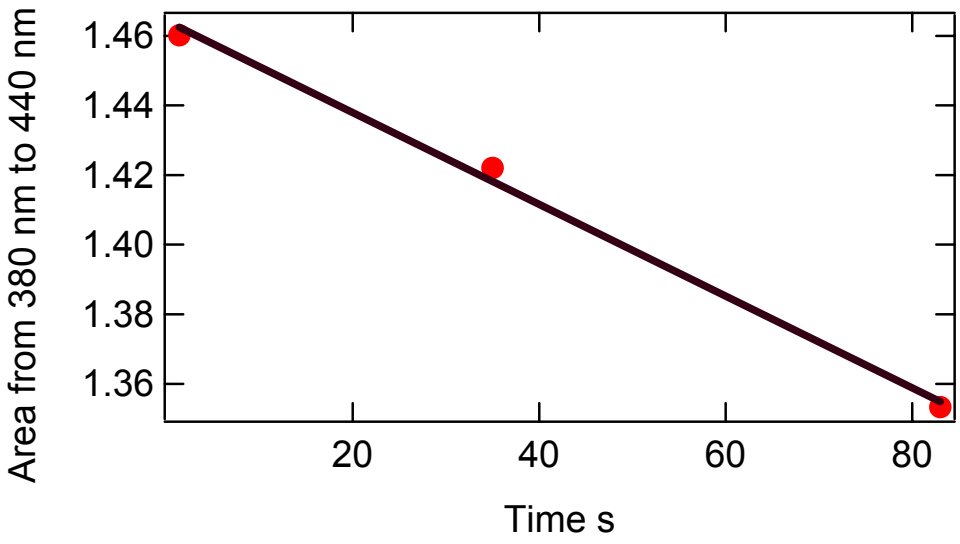


Figure 3.22 Graph of the area between 380 nm and 440 nm that lies under the Soret band for HRP vs. seconds after addition of 1000 molar excess of peroxide was added to the protein solution.

Hydrogen peroxide susceptibility test of HHMb showed a third very different response to excess peroxide. In Figure 3.23 the initial spectrum of HHMb was taken before the addition of peroxide (red trace). The black trace was taken 32 s after 1000M excess of peroxide was added. Since degradation of HHMb occurred rapidly, we chose to inspect HHMb at lower peroxide concentrations.

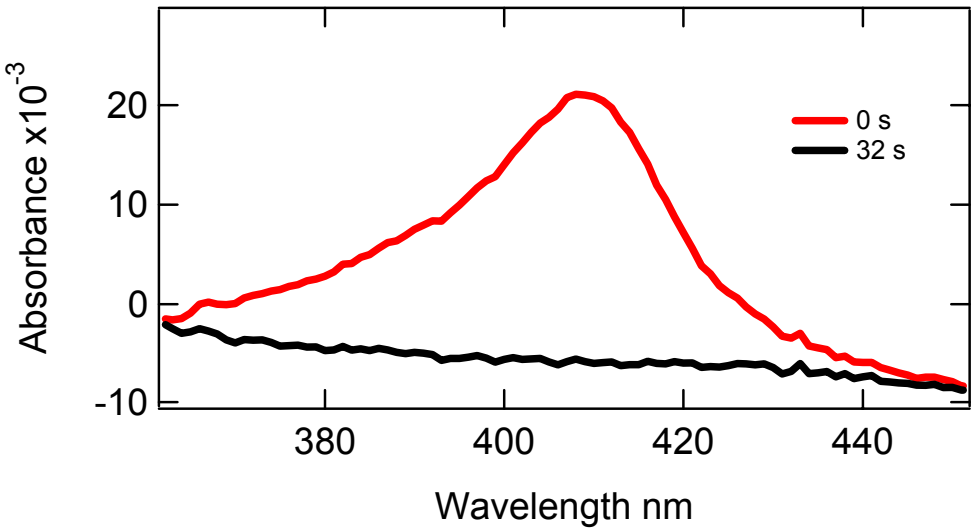


Figure 3.23 Assay of hydrogen peroxide susceptibility test on HHMb to probe HHMb's tolerance to excess peroxide.

In Figure 3.24 the initial spectrum of HHMb showed the Soret maximum to be at 407 nm (red trace). Five seconds after the addition of 100 fold excess peroxide, the Soret band decreased in intensity, but the maximum remained constant at 407 nm (orange trace). Eight seconds after the start of the reaction, a shift in the Soret maximum and broading of the line shape (light orange trace) was observed. At 11 seconds we noticed the Soret band had a maximum at 422 nm (green trace). The Soret maximum remained at 422 nm up to 98 seconds, with the only noticeable change being the decrease of the left shoulder (blue trace).

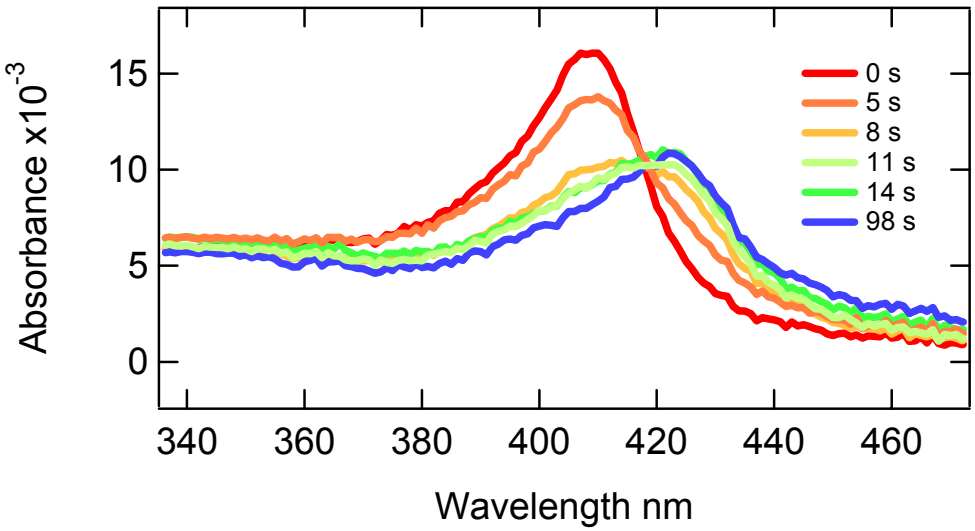


Figure 3.24 Hydrogen Peroxide susceptibility test on HHMb to probe HHMb tolerance to excess peroxide.

Once again we chose to look at the area under the Soret band, instead of a single wavelength for an indicator of how much intact HHMb was present at different times. We chose to define the Soret band from 340 nm to 440 nm. When we calculated the area under the Soret band between 340 nm and 440 nm and graphed the area vs. time, we obtained Figure 3.25. In this figure the degradation of HHMb was erratic. Once again this was a different response than what was obtained for 6x His DHP and a different response than that which was obtained for HRP. Addition of 100 molar excess of peroxide to HHMb resulted in rate 3.0 x $10^{-5}$ μM of HHMb degraded per second per μM of peroxide.

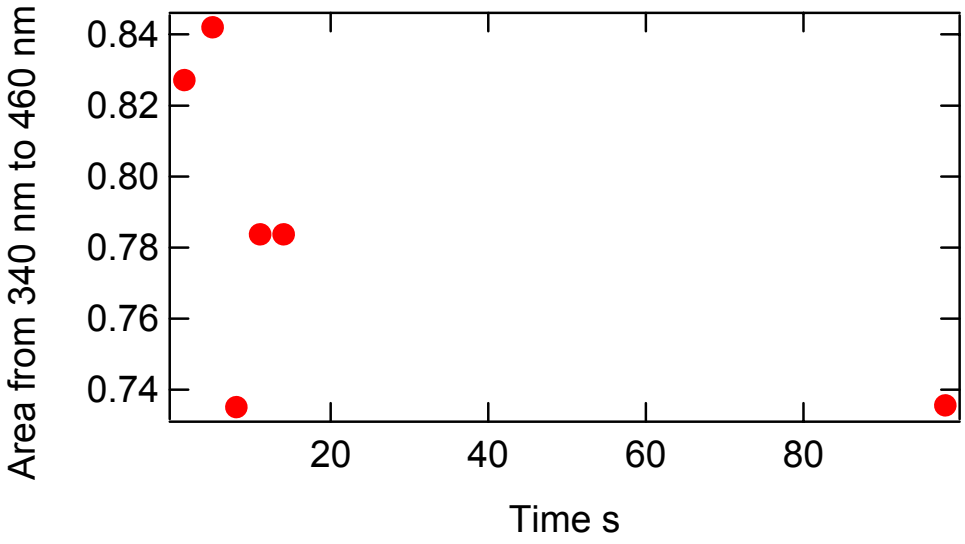


Figure 3.25 Graph of the area between 340 nm and 460 nm that lies under the Soret band for HHMb vs. seconds after addition of 1000 molar excess of peroxide was added to the protein solution.

**3.6 Stopped-Flow Assays Results**

Figures 3.26 and 3.27 showed stopped-flow assays of 6x His DHP and HRP. In Figure 3.26 consumption of substrates was monitored at 316 nm. The appearance of product was monitored at 272 nm in Figure 3.27. HRP was represented in the solid traces and 6x His DHP is represented in the dashed traces. Table 3.2 contains the terms used in the exponential fits of the traces in Figures 3.26 and 3.27. The exponential equation was $y = A \exp(-kt)$.

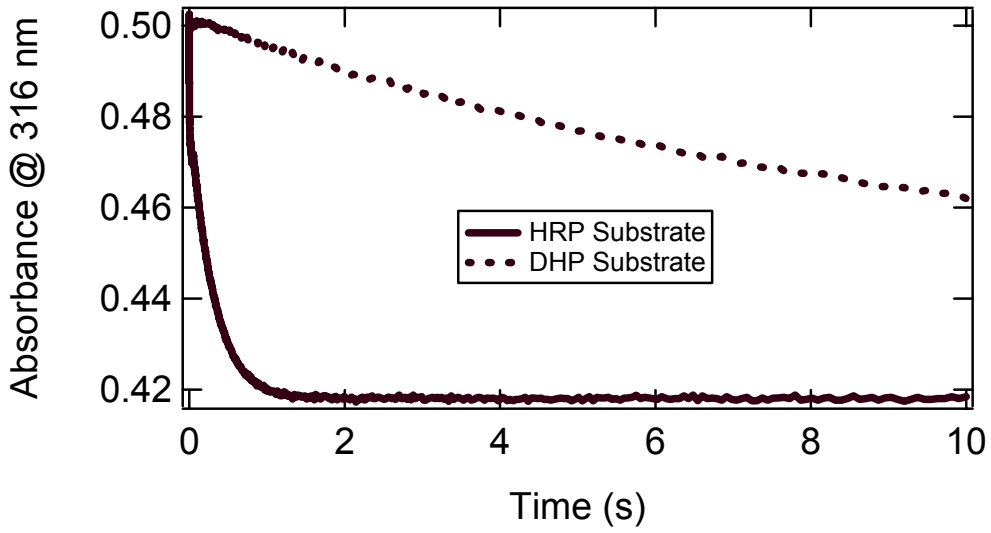


Figure 3.26 Stopped-flow experiment monitoring the consumption of 2,4,6-tribromophenol at 316 nm by HRP (solid line) and 6x His DHP (dashed line). Assay conditions were 20 mM potassium phosphate pH 6.0, 0.1 M $KNO_3$, 12 μM enzyme, and 11 μM $H_2O_2$.

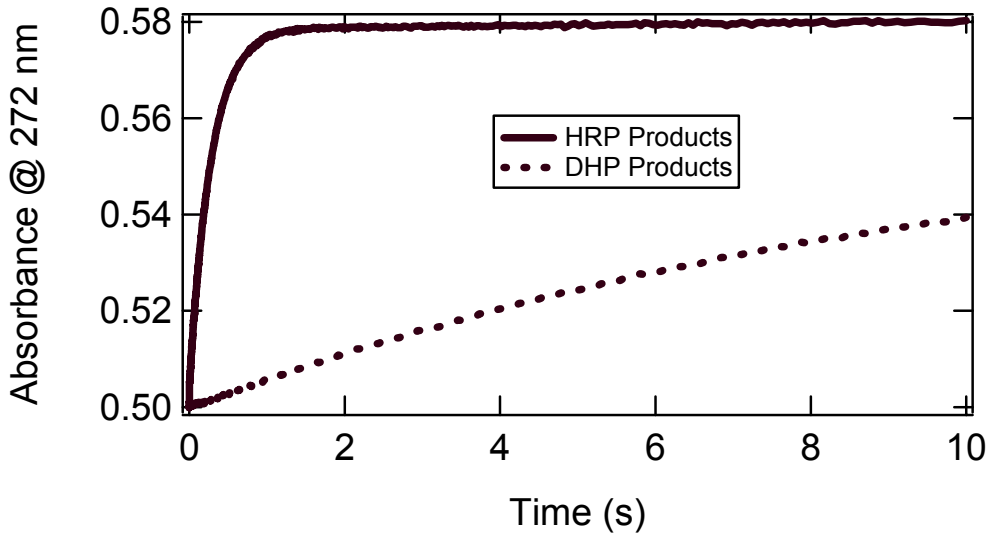


Figure 3.27 Stopped-flow experiment monitoring the grow-in of products at 272 nm by HRP (solid line) and 6x His DHP (dashed line). Assay conditions were 20 mM potassium phosphate pH 6.0, 0.1 M $KNO_3$, 12 μM enzyme, and 11 μM $H_2O_2$.

| Wavelength | Enzyme | y | A | k | Turnover # |
|---|---|---|---|---|---|
| 316 nm | 6x His DHP | 0.42297 | 0.77434 | 0.070127 | 3.00 |
| 316 nm | HRP | 0.57867 | -0.076449 | 3.6519 | 138 |
| 272 nm | 6x His DHP | 0.56742 | -0.067414 | 0.088627 | 3.00 |
| 272 nm | HRP | 0.41831 | 0.064612 | 3.5505 | 123 |

Table 3.2 Exponential fits of the traces in figure 3.24 and 3.25 results and approximate turnover numbers. Turnover numbers have units of μmole of substrate or product * μmole of enzyme$^{-1}$ * s$^{-1}$.

**3.7 Conclusions**

UV-vis spectroscopic assays of DHP and 6x His DHP show that both recombinant forms of dehaloperoxidase were active on 2,4,6-triflorophenol, 2,4,6-trichlorophenol, 2,4,6-tribromophenol and 2,4,6-triiodiophenol. Both recombinant enzymes were yield products that had the same UV-Vis characteristics on the same time scale. The major difference that was observable in the UV-Vis assays of DHP and 6x His DHP was the shift that has been identified in the heme degradation. The nature of this difference between the two recombinant forms of dehaloperoxidase requires further investigation. Due the speed of the degradation, this study should be done as a stopped-flow experiment. Degradation do to addition of 1000 molar excess peroxide was negligible for HRP. Degradation do to addition of 1000 molar excess peroxide was complete and immediate for HHMb. Degradation do to addition of 1000 molar excess peroxide resulted in 5.7 x $10^{-6}$ μM 6 x His DHP per second per μM peroxide.

Stopped flow analysis of 6x His DHP and HRP has shown us that HRP was 52 times faster than 6x His DHP at the consumption of 2,4,6-tribromophenol and 40 times faster at

generating product. The stopped flow study also showed us that the time resolution on our UV-Vis instrument was sufficient to continue studies of 6x His DHP, but not for HRP.

Since the results of the peroxide susceptibility of DHP resembled that of myoglobin, it would indicate that dehaloperoxidase may not use peroxide as a native cofactor. Instead of peroxide, dehaloperoxidase may have used a flavoprotein that aided in the electron and proton transfer to the heme that had oxygen bound in the sixth coordination site. Such electron and proton transfer in the presence of oxygen is known in the chemistry of cytochrome P450's and the use of a flavoprotein is required for function of chloroperoxidase form *Notomastus lobatus,* the only other known heme peroxidase with a globin fold.

In the literature, dehaloperoxidase was reported to produce a haloquinone product. The haloquinone would result from a two electron transfer from the trihalogenated phenol. We have not been able to isolate this product, but if true, then the standard mechanism for peroxidase cycle would apply to dehaloperoxidase, since the excepted cycle had two one electron transfer steps due to rapid diffusion of substrate and product. Breaking from the excepted paradigm seemed appropriate in the case of dehaloperoxidase, since dehaloperoxidase had an actual binding site for substrate that HRP did not. This site could act as a cage that traps the substrate long enough for a two electron transfer to occur.

The assays in this thesis represented an attempt to understand the mechanism of dehaloperoxidase. Much more work needs to be done, but conditions for future studies using the stopped-flow approach to determine rate constants has been established and are currently being worked on as well as attempts to isolate and characterize compound I. We are attempting to isolate assay products via LC-MS and GC-MS. We are also probing the use of electrochemistry to facilitate reactions without the use of peroxide. Work in its area is

ongoing and much of the methods development portion of the assay studies has already been established in this document.

## References


16. H. Brian Dunford, Heme Peroxidases, Wiley-VCH, New York, 1993
17. Hewson, WD., and Dunford, HB., Journal of Biological Chemistry, 1976; **251**: 6036-6042.
18. Zhang E, Chen YP, Roaach MP, et al. Crystallization and initial spectroscopic characterization of the heme-containing dehaloperoxidase from the marine polychaete *Amphtrite ornate* . Acta Cryst. 1996; **D52**: 1191-1193.
19. Chen YP, Woodin SA, Lincoln DE, Lovell CR. An unusual dehalogenaating peroxidase from the marine terebellid polychaete *Amphirite ornate*. J. Biol.Chem. 1996; **271**: 4609-4612.
20. Roach, MP., Chen, YP., and Dawson, JH., *Notomastus lobatus* chloroperoxidase and *Amphirite ornata* dehaloperoxidase both contain histidine as their proximal heme iron ligand Biochemistry, 1997; **36**: 2197-2202
21. Goodin DB, McRee DE. The Aspp-His-Fe Triad of cytochrome c peroxidase controls the Reduction Potential, Electronic Structure, and Coupling of the Tryptophane Free Radical to the Heme. Biochemistry 1993; **32**: 3313-3324.
22. W. W. Clealand, The Enzymes, 3rd edition, P. D. Boyer, ed; Academic, New York, 1970, Vol II.

# Chapter 4 CO Recombination as a Function of Temperature

## 4.1 Introduction

Myoglobin has been the model system for protein structure-dynamics-function studies for greater than 40 years[1]. Crystal structures show a pattern of eight α- helixes surrounding a heme prosthetic group. Ligands that bind to the heme must find a way though the helixes to either enter into the protein interior and bind to the heme or to escape from the globin[2]. Detailed research on the mechanism of ligand binding seems to have prompted more questions that it has answered. The idea that ligand binding is a one step process had to be modified when the non-exponential internal recombination and multistep kinetics gave an insight to a more complicated ligand binding process [3].

Recently myoglobin has been studied using x-ray crystallography of photoproducts, time-resolved spectroscopy and protein engineering. These studies have shown that photolyzed ligands which reside close to the heme in the primary docking site B. Two more internal cavities have been identified as C and D, are both occupied by photolized CO ligands. There are a total of four sites that are large enough to hold a Xe atom, and with recent experiments it has been shown that these sites are responsible for both ligand capture and escape [1-6].

We have combined Fourier transform inferred spectroscopy with cryogenic temperatures and photolysis to probe the CO recombination of 6x His DHP. The purpose of these experiments is to explore of electrostatics and steric hindrance of the ligand binding pocket as well as the docking sites the ligand occupies after photolysis. Globins have highly conserved histidine 64 residues and valine 68 residues on their distal side. Dehaloperoxidase has both histidine and valine residues except they are in an alternate orientation with the valine closer to the heme than the histidine residue. Since both the histidine and valine

residues have been shown to be part of the overall kinetic barrier to ligand binding, in myoglobin systems, we believe dehaloperoxidase would be very interesting to study using this method[1-5].

The imidazole side chain of the histidine 64 in myoglobin is protonated at low pH. The protonated state causes the residue to swing toward the solvent to better solvent the positive charge which results in the open conformation that has been associated with Ao. Ao is characterized by an apolar pocket and in myoglobin appears at ~1965 $cm^{-1}$. The closed conformation is related to $A_1$ and $A_3$, at ~1945 and ~1933 $cm^{-1}$, where the positive partial charge of the Nε–H of the histidine 64 imidazole interacts electrostatically with the bound CO. Opposite orientations of the CO molecule with respect to the heme have been associated with $B_2$ and $B_l$ at 2119 and 2131 $cm^{-1}$. $B_o$, 2150 $cm^{-1}$, represents CO ligands at site B in the $A_3$ conformation with a strong interaction with histidine 64 in the unbound state[1].

**4.2 Methods**

Sample preparations- Protein was purified from *E. coli* as previously described in this thesis. IR samples were prepared so that the final concentration of buffer was 10 mM potassium phosphate at pH of 7.0 or 4.0. Glycerol was used in the IR samples as a cryoprotectant at 50% (v/v). Protein solutions of buffer and glycerol were purged with nitrogen gas to remove oxygen. Then the sample was reduced with 1M sodium dithionite to yield a ferric sample by adding a trace of the dithionite to the oxygen free sample. The ferric sample was then purged with CO gas to generate the bound CO ligand.

FTIR and Cryogenic Setup- A few microliters of the protein solution were placed between two $CaF_2$ or ZnSe windows separated by a 25 μm spacer. The windows were sandwiched together using a copper sample mount which was placed into a Janis St-100 or

Oxford R.5456.4 cold finger, equipped with a temperature sensor and digital temperature controller. Data was collected using a Bio-Rad FS 3000x FTIR bench with Bio-Rad Win-Pro IR version 2.97software at 2 $cm^{-1}$ resolution. The bench was purged with dry air to remove water vapor before and during data collection.

Data collection method- Once a sample was loaded into the cold finger and placed in the bench, a few minutes were allowed for purging of the spectrometer with a dry air line to remove water vapor. Several spectra were taken at room temperature before helium transfer started. Once the helium transfer started temperature was monitored until it reached ~80 K when the cold finger was evacuated by vacuum. Temperatures of 5K were reached and held constant during the collection of data that represented the pre photolysis data set. The CO ligand was then photolyzed by a Minilite, Yd-YAG, until the CO peak was no longer present in the sample (5-15 minutes). The temperature was then allowed to warm slowly. The temperature was held constant or allowed to vary only 1K during data collection at various temperatures.

**4.3 Results**

Data were collected and initially analyzed using Bio-Rad's Win-Pro IR v2.97. Once all data were collected all spectra were ratioed to a background spectrum consisting of windows without protein. The data that resulted was in absorbance. Next, the data were baseline corrected in Win-Pro v2.97 and finally imported into Wavematrix Igor 5.0. The following figures 4.1-4.15 are examples of the data collected in this experiment. From these figures we were able to determine the stretching frequency for the CO or A states, and B bands.

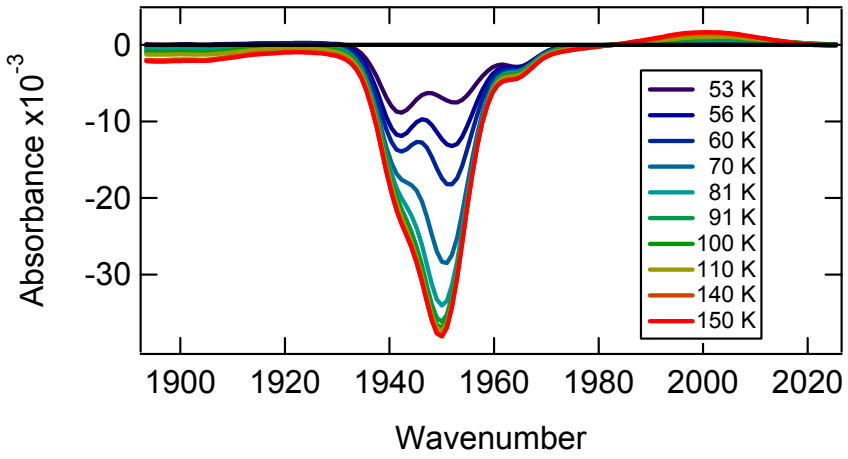


Figure 4.1 DHP-CO pH 7.0 $\nu_{C-O}$ or A states are located at 1966 1950, and 1942 $cm^{-1}$. Spectra graphed from blue to red where blue is the lowest temperature and red is the highest temperature. Notice the population shift form 1942 $cm^{-1}$ to 1950 $cm^{-1}$ as the temperature increases.

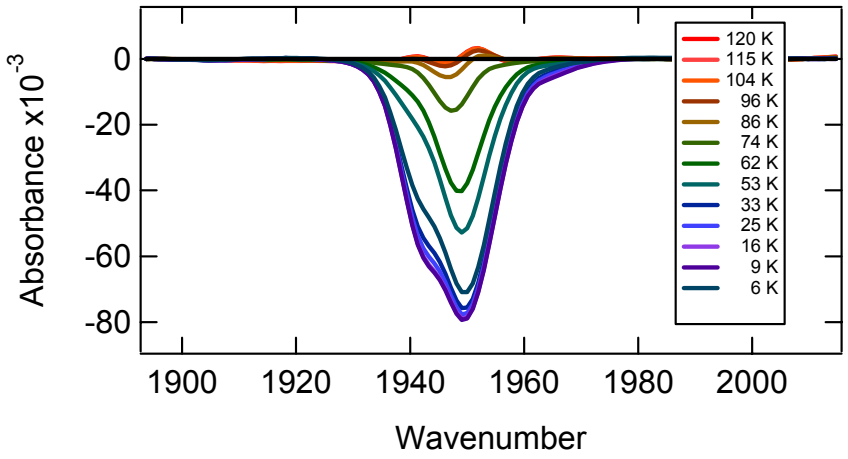


Figure 4.2 DHP-CO with TBP pH 7.0 $\nu_{C-O}$ or A states are located at 1951 $cm^{-1}$ and 1942 $cm^{-1}$. Notice that the peak located at 1942 $cm^{-1}$ is present at lower temperatures but disappears as temperature increases.

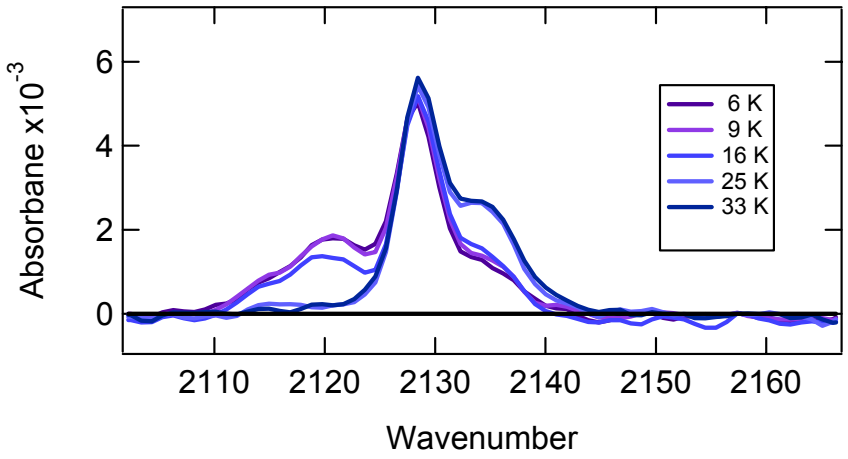


Figure 4.3 DHP-CO with TBP pH 7.0 shows the B bands as 2120 $cm^{-1}$,2128 $cm^{-1}$ and 2135 $cm^{-1}$. Notice the shift from 2120 $cm^{-1}$ at lower temperatures to 2135 at higher temperatures with the near constant peak at 2128 $cm^{-1}$.

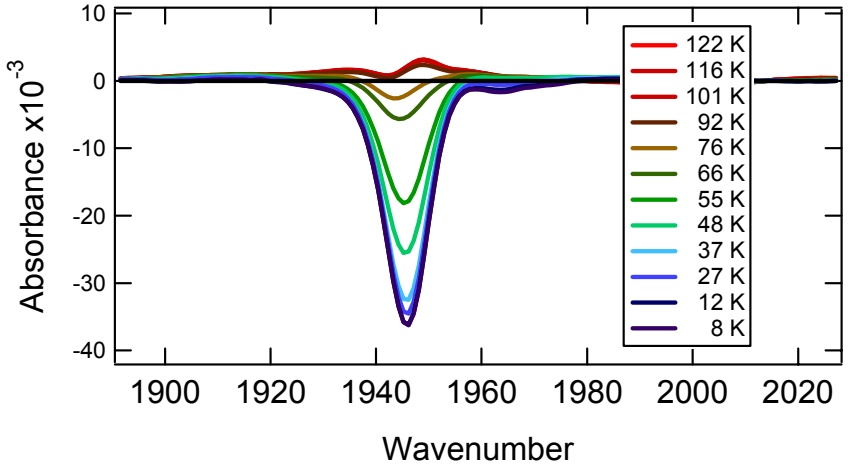


Figure 4.4 HHMb-CO pH 7.0 shows $\nu_{C\text{-}O}$ or A states are located at 1946 $cm^{-1}$ and there is no shifting with temperature.

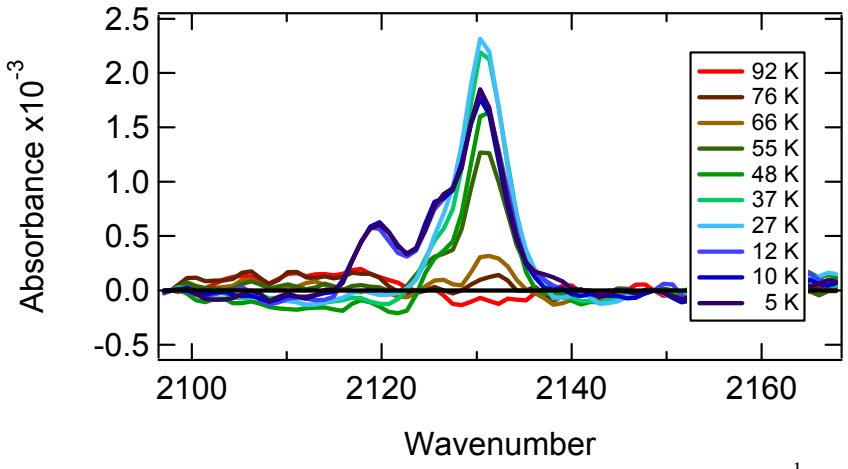


Figure 4.5 HHMb-CO pH 7.0 shows the B bands as 2120 $cm^{-1}$ and 2130 $cm^{-1}$. Notice the band at 2120 $cm^{-1}$ disappears at higher temperatures.

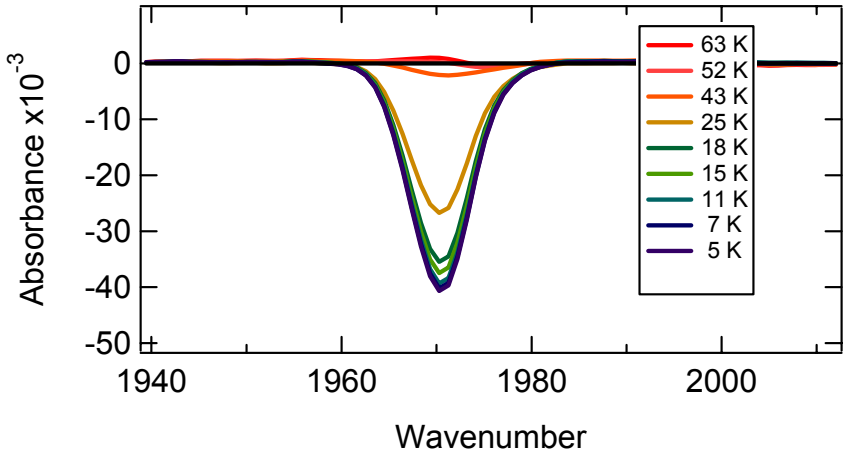


Figure 4.6 H64V-CO pH 7.0 CO shows $\nu_{C\text{-}O}$ or A states are located at 1970 $cm^{-1}$ and there is no shifting with temperature.

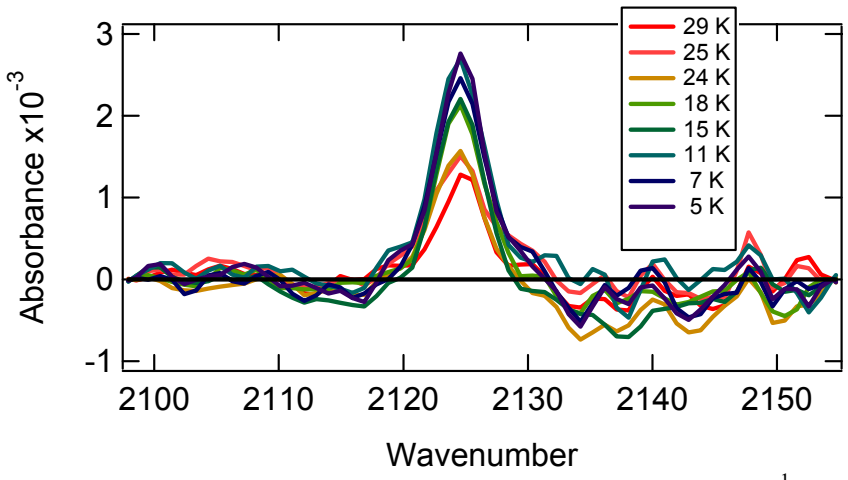


Figure 4.7 H64V-CO pH 7.0 shows the B bands as 2119 $cm^{-1}$ 2125 $cm^{-1}$ and 2130 $cm^{-1}$. Notice the band at 2130 $cm^{-1}$ disappears at higher temperatures.

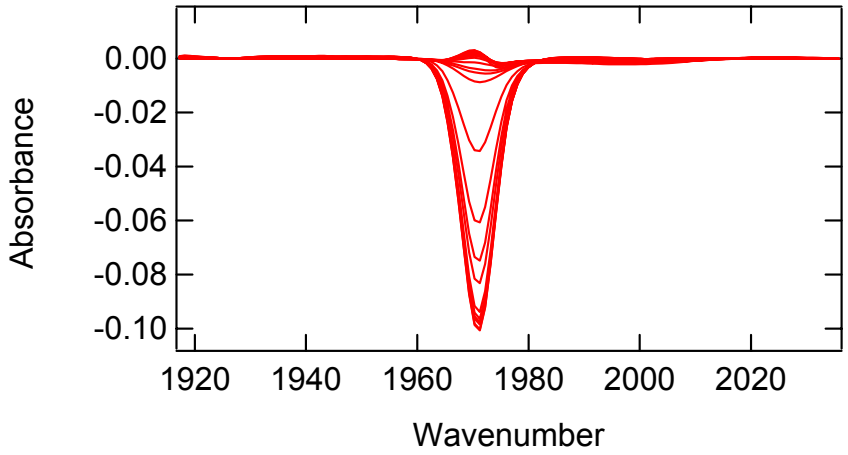


Figure 4.8 H64V-CO with TBP pH 7.0 shows $\nu_{C\text{-}O}$ or A state is located at 1971 $cm^{-1}$.

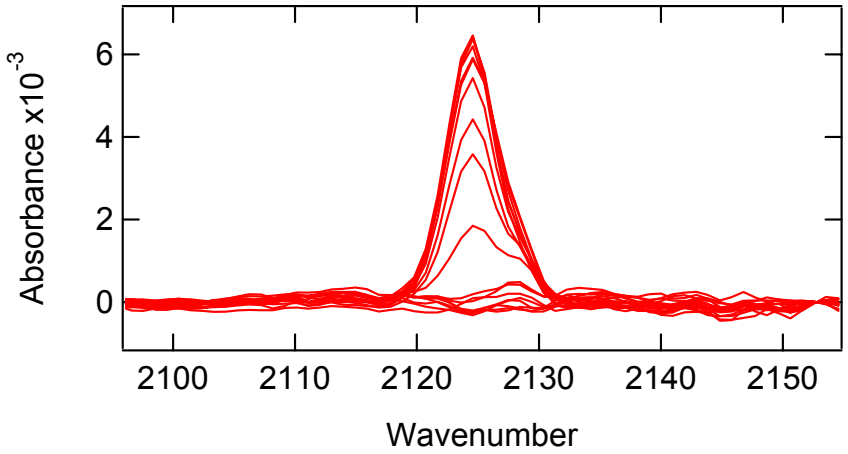


Figure 4.9 H64V-CO with TBP pH 7.0 shows the B bands as 2119 $cm^{-1}$ and 2128 $cm^{-1}$. Notice the band at 2128 $cm^{-1}$ appears at higher temperatures.

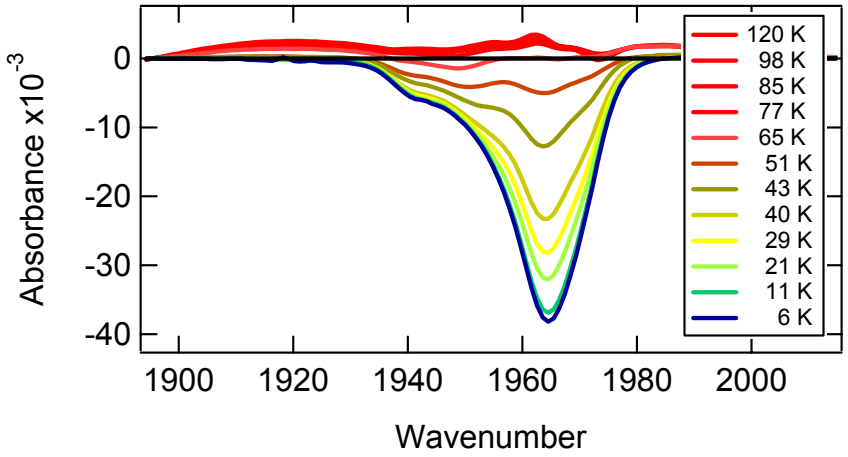


Figure 4.10 DHP-CO pH 4.0 $\nu_{C\text{-}O}$ or A states are located at 1972 cm$^{-1}$, 1965 cm$^{-1}$, 1950 cm$^{-1}$ and 1941 cm$^{-1}$. Notice that the peak at 1965 cm$^{-1}$ is the dominate peak at all temperatures but at higher temperatures the distribution between the peaks start to even out.

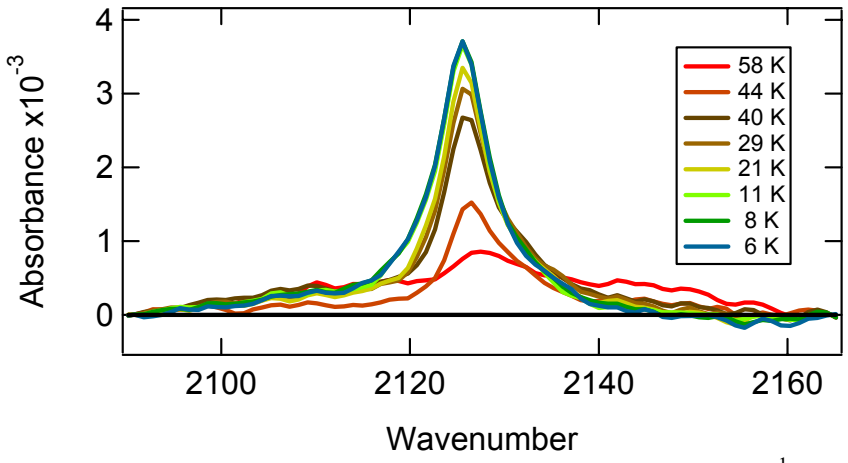


Figure 4.11 DHP-CO pH 4.0 shows the B bands at 2132 cm$^{-1}$ and 2127 cm$^{-1}$. The band at 2127 cm$^{-1}$ appears as the temperature increases making the peak at 2132 cm$^{-1}$ look broad and heavily shouldered.

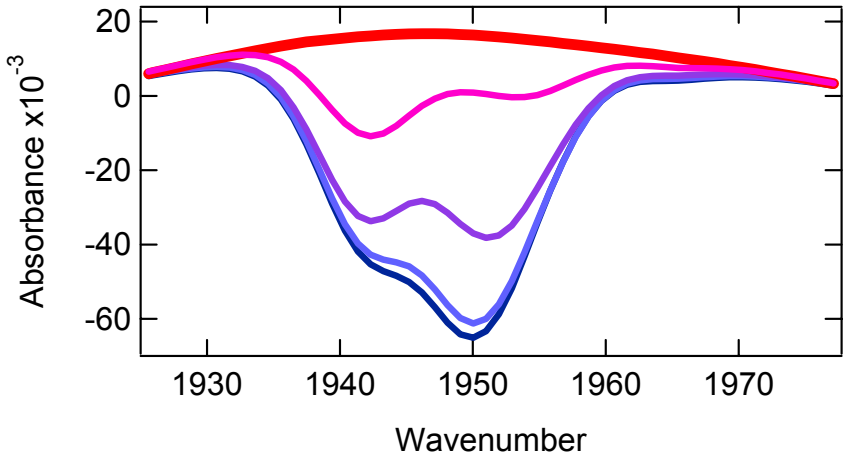


Figure 4.12DHP-CO with TBP pH 4.0 $\nu_{C\text{-}O}$ or A states are located at 1951 $cm^{-1}$, 1942 $cm^{-1}$. There a sift form 1951 $cm^{-1}$ to 1942 $cm^{-1}$ as temperature increases.

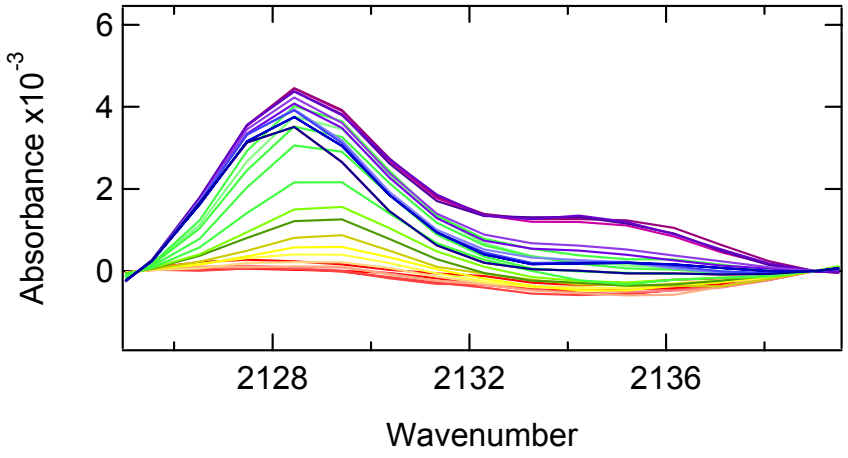


Figure 4.13 DHP-CO with TBP pH 4 shows the B bands at 2128 $cm^{-1}$ and 2135 $cm^{-1}$.

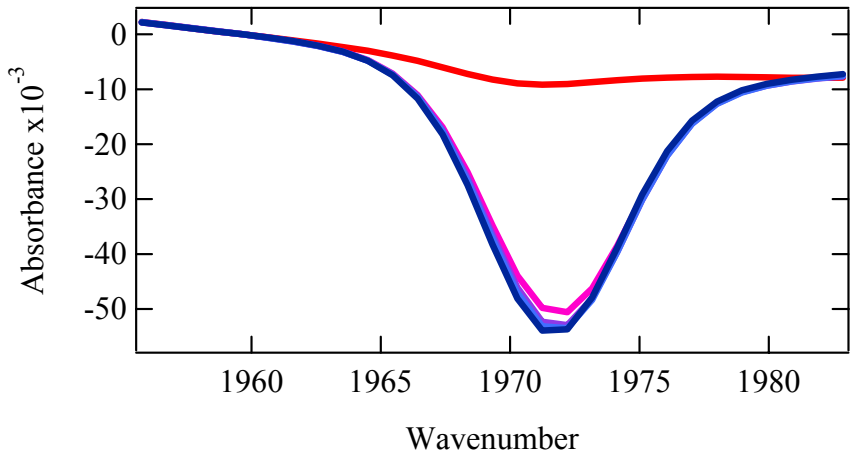


Figure 4.14 H64V-CO pH 4.0 $\nu_{C\text{-}O}$ or A state is located at 1972 $cm^{-1}$. There is not shift with temperature of the A state for H64V-CO at pH 4.0.

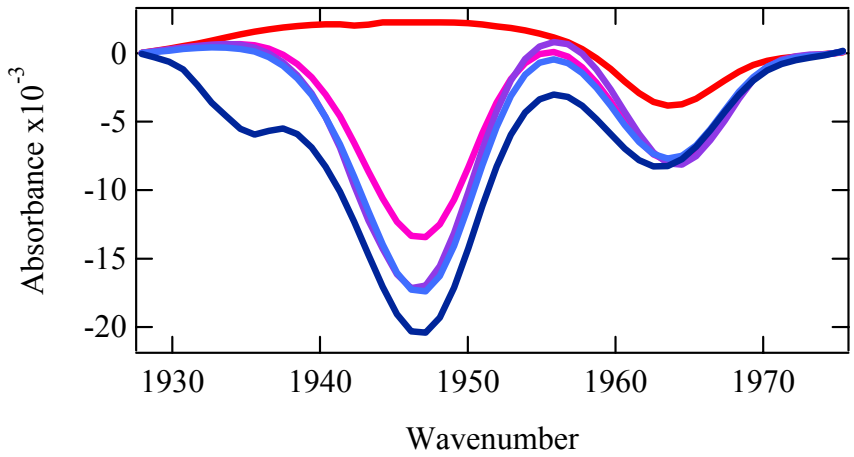


Figure 4.15 HHMb-CO pH 4.0 $\nu_{C\text{-}O}$ or A states are located at 1964, 1947, and 1935 $cm^{-1}$. The band at 1935 $cm^{-1}$ appearance as temperature increases and at the lower temperatures it is not present. Note the highest temperature is in blue and the lowest temperature is in red.

**4.4 Discussion**

CO bound to the heme is represented as the A1 state. Several A states (Ao, $A_1$, $A_3$, $A_I$, and $A_{II}$) have been identified in myoglobin and its mutants. After photolysis the CO ligand can occupy several different sites with in the protein. The primary photoproduct site is B, some times called the primary docking site, and is the nearest location that a free CO molecule can occupy. When a CO molecule is in site B it is parallel to the heme. Primary

photoproduct B occurs at one location but two infrared bands is typically observed. The two bands are due to opposite orientations for the carbon monoxide molecule, CO vs. OC. The opposite orientations of the carbon monoxide dipoles give rise to Stark splitting. Stark splitting has been observed for each photoproduct site. When photolysis occurs at very low temperatures the freed CO molecule is restricted to the B state (see Figures 4.16-4.18). As temperature increases so does the fluxuations in the protein. The fluxuations will allow the free CO to migrate to additional sites within the protein scaffold. The Xe4 cavity or C state is the site that will populate next as temperature increases. The C state is blocked by L29 in myoglobin and L25 in DHP. As the temperature increases these residues swing out allowing the CO molecule to diffuse in. Once the CO is in the C state a frequency shift is observed. Additional increase in temperature permits residue I107 in myoglobin and residue I100 in DHP to move back allowing CO to migrate from Xe4 to Xe2. CO will not remain in the Xe2 site. Once in the Xe2 site the CO can return to the Xe4 site or proceed to the Xe1 or D state. Xe1 is located on the distal side of the heme. In order for a ligand to escape to the solvent from the heme it must migrate through each of the docking sites A, B, C, and D the reverse trip must be traveled for a ligand to be bound from the solvent to the heme. The fluxuations in the protein that allow for ligand migration result in the entropy barriers that must be overcome in order for bind and dissociation to occur.

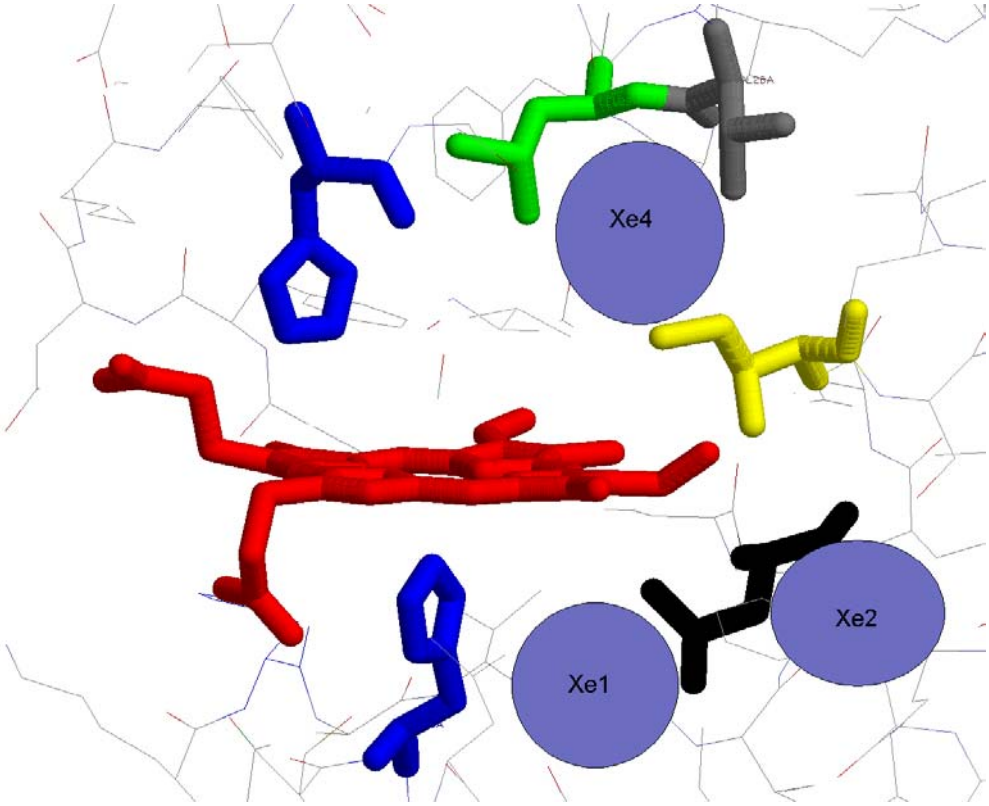

Figure 4.16 show the Xe binding sites in HHMb. The distal side of the heme is on top.

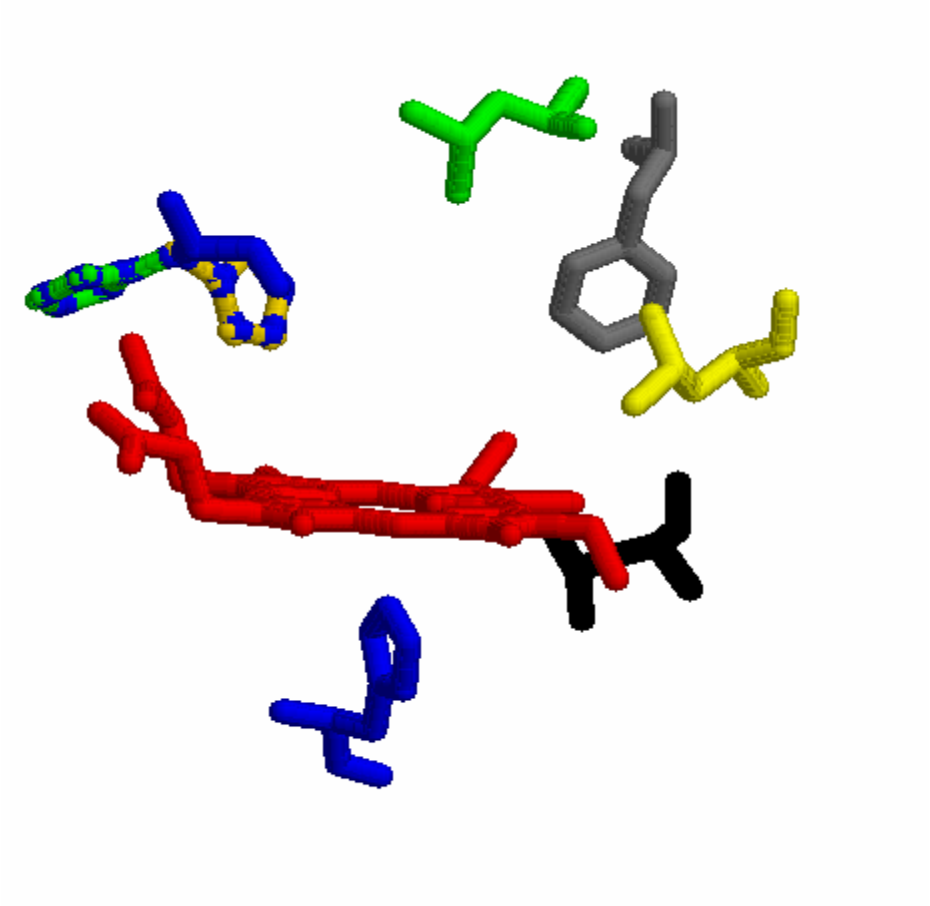

Figure 4.17 show the heme environment of DHP that is predicted to be responsible for the ligand migration into Xe binding sites. Note the distal side of the heme is up and the blue/green/mustard residue represents the distal histidine in two equally populated orientations.

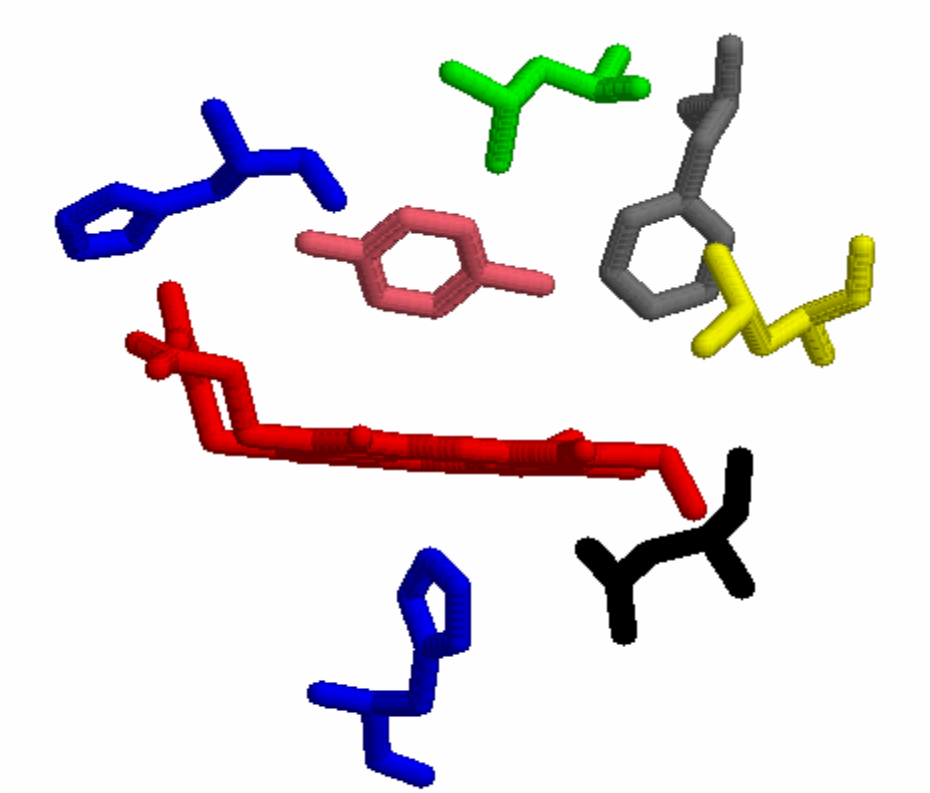

Figure 4.18 show the heme environment of DHP with substrate bound that is predicted to be responsible for the ligand migration into Xe binding sites. Note the distal side of the heme is up and the blue residues are histidines and the pink aromatic is the substrate.

In figure 4.1 DHP-CO pH 7.0 $\nu_{C-O}$ or A states are located at 1966, 1950, and 1942 $cm^{-1}$. Notice the intensity shift from 1942 $cm^{-1}$ to 1950 $cm^{-1}$ as the temperature increases. This could indicate motion of distal side residues moving as temperature increases. This also indicates that the lower temperatures are locking the protein into conformations that restrict the motions around the CO ligand.

In Figure 4.2 DHP-CO with TBP pH 7.0 $\nu_{C-O}$ or A states are located at 1951 $cm^{-1}$ and 1942 $cm^{-1}$. The peak located at 1942 $cm^{-1}$ is not present at lower temperatures but grows as temperature increases. This is similar to the shift that is seen in DHP-CO pH 7.0 difference spectra with and without the substrate, TBP. In figure 4.3 DHP-CO with TBP pH 7.0 shows

the B bands as 2120 $cm^{-1}$,2128 $cm^{-1}$ and 2135 $cm^{-1}$. There is a shift from 2120 $cm^{-1}$ at lower temperatures to 2135 $cm^{-1}$ at higher temperatures with the near constant peak at 2128 $cm^{-1}$.

In figure 4.4 HHMb-CO pH 7.0 shows $\nu_{C-O}$ or A states are located at 1946 $cm^{-1}$ and there is no shifting with temperature. In figure 4.5 HHMb-CO pH 7.0 shows the B bands as 2119 $cm^{-1}$ and 2130 $cm^{-1}$. The band at 2120 $cm^{-1}$ disappears at higher temperatures without an additional band appearing.

In figure 4.6, 4.8, there are no temperature-dependent shifts in A states of H64V-CO pH 7.0 either with or without TBP. However the B bands of these samples do change with increasing temperature. In figure 4.7 H64V-CO pH 7.0 shows the B bands as 2119 $cm^{-1}$ 2125 $cm^{-1}$ and 2130 $cm^{-1}$. The band at 2130 $cm^{-1}$ disappears at higher temperatures. In figure 4.9 H64V-CO with TBP pH 7.0 shows the B bands as 2119 $cm^{-1}$ and 2128 $cm^{-1}$. The band at 2128 $cm^{-1}$ appears at higher temperatures.

In figure 4.10 DHP-CO pH 4.0 $\nu_{C-O}$ or A states are located at 1972 $cm^{-1}$, 1965 $cm^{-1}$, 1950 $cm^{-1}$ and 1941 $cm^{-1}$. The peak at 1965 $cm^{-1}$ is the dominate peak at all temperatures but at higher temperatures the distribution between the peaks start to even out. In figure 4.12DHP-CO with TBP pH 4.0 $\nu_{C-O}$ or A states are located at 1951 $cm^{-1}$, 1942 $cm^{-1}$. There a sift form 1951 $cm^{-1}$ to 1942 $cm^{-1}$ as temperature increases.

Figure 4.11 shows the B bands of DHP-CO pH 4.0 at 2132 $cm^{-1}$ and 2127 $cm^{-1}$. The band at 2127 $cm^{-1}$ appears as the temperature increases making the peak at 2132 $cm^{-1}$ look broad and heavily shouldered. Figure 4.13 DHP-CO with TBP pH 4 shows the B bands at 2128 $cm^{-1}$ and 2135 $cm^{-1}$ with no changes due to temperature.

In figure 4.14 H64V-CO pH 4.0 $\nu_{C-O}$ or A state is located at 1972 $cm^{-1}$. There is not shift with temperature of the A state for H64V-CO at pH 4.0. Figure 4.15 HHMb-CO pH 4.0

$\nu_{C-O}$ or A states are located at 1964, 1947, and 1935 $cm^{-1}$. The band at 1935 $cm^{-1}$ appearance as temperature increases and at the lower temperatures it is not present.

The temperature where 90% of the population has recombined, protein with the bound CO ligand, can be determined by graphing the maximum absorbance of the CO or A state that dominates the population vs. the temperature of the sample when the absorbance was measured. This allows us to decide if it substrate and/or pH has a role in the recombination of the CO ligand, Figure 4.19.

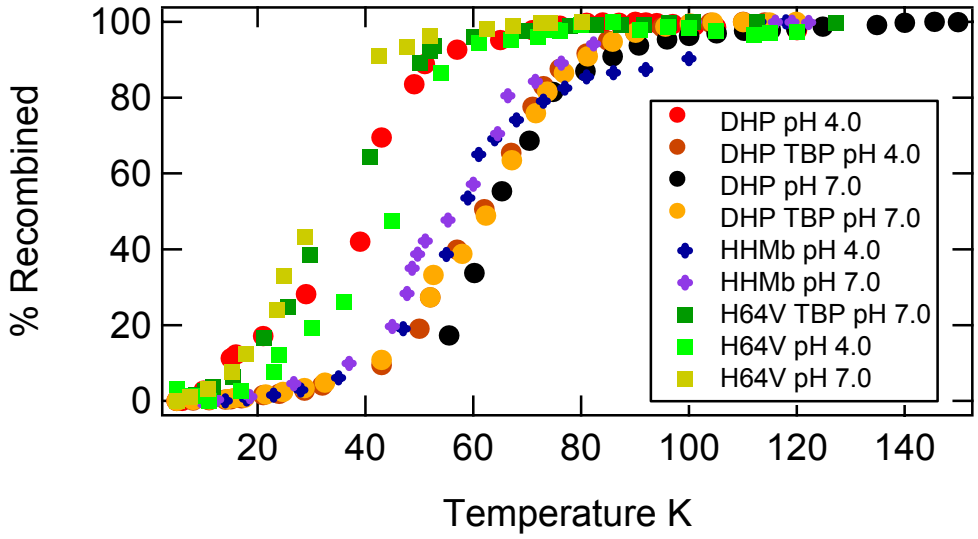


Figure 4.19 Percent of CO ligand recombination of as a function of temperature.

| Sample | $\nu_{C-O}$ or A ($cm^{-1}$) | B bands ($cm^{-1}$) | **90% Recombine. Temp K** |
|---|---|---|---|
| DHP pH 4.0 | 1972, **1965**, 1950, 1941 | 2132, **2127** | 54 |
| DHP pH 7.0 | 1966, **1950**, 1942 | **2128** | 83 |
| DHP + TBP pH 4.0 | **1951**, 1942 | 2135, **2128** | 79 |
| DHP + TBP pH 7.0 | **1949**, 1943 | **2128**, 2121 | 81 |
| H64V pH 4.0 | **1972** | 2129, **2125**, 2118 | 57 |
| H64V pH 7.0 | **1971** | 2130,**2125**, 2119 | 42 |
| H64V + TBP pH 7.0 | **1971** | 2128, **2125** | 51 |
| HHMb pH 4.0 | 1964, **1947**, 1935 | **2130**, 2119 | 89 |
| HHMb pH 7.0 | **1946** | **2130**, 2127, 2120 | 77 |

Table 4.1 Table of the A bands, B band and temperature where 90% of the CO recombines with the protein. Bold wavenumbers are the most populated.

**4.5 Conclusion**

The A states and B bands for dehaloperoxidase have been identified at two different pH's, with and without substrate, (2,4,6-tribromophenol) as well as the temperature where 90% of the photolyzed ligand recombines see table 4.1. We were able to identify shifts in populations in both the A states and B bands as a function of temperature. We have plans to continue theses studies.

Horse heart myoglobin agrees with sperm whale myoglobin as presented in literature[1-5]. HHMb was used as a control in all experiments due to its availability. The sperm whale myoglobin mutant H64V has the distal histidine, residue 64, replaced with a valine. The H64V mutation simulates the distal residue in dehaloperoxidase thus was chosen as a comparison. DHP shows substantial differences both at pH 7.0 and pH 4.0. Substrate binding can be detected with a functional shift of the CO frequency. The role of the multiple bands in DHP remains to be investigated.

A UDR filter was not used and should have been. The use of a UDR filter would have prevented photolysis of CO due to the HeNe laser present in the bench. Since a UDR filter was not used some of the CO was photolized before the use of the Yd-YAG. This

means my dark sample, sample that should represent no CO photolysis, was not a true dark sample. In addition to this we have learned that each difference spectra should be a difference between the photolyzed sample and the dark sample at the same temperature. The need for multiple dark samples is to avoid getting a positive feature in the difference spectra. We did get positive features in our experiments do to using only one the dark sample at 4K for all calculations.

## References


1. Nienhaus, K., Deng, P., Olson, J., Warren, J., and Nienhaus, G. U., (2003) *The Journal of Biological Chemistry*, 278, 42532-42544
2. Nienhaus, K., Deng, P., Olson, J., Kregl, J., and Nienhaus, G. U., (2003) *Biochemistry*, **42**, 9633-9646
3. Nienhaus, G. U., Muller, J. D., McMahon, B. H., Frauenfelder, H., (1997) *Physica D*, **107**, 297-311
4. Nienhaus, K., Deng, P., Olson, J., Kregl, J., and Nienhaus, G. U., (2003) *Biochemistry*, **42**, 9647-9658
5. Nienhaus, G. U., Chu, K., and Jesse, K., (1998) *The Journal of Biological Chemistry*, **278**, 42532-42544

# Chapter 5: Transient Absorption Experiments to Probe Glycerol Concentration and Substrate Binding Effects on the NO Rebinding Kinetics of Dehaloperoxidase

## 5.1 Introduction

Transient absorption experiments were performed to probe the effects of increasing glycerol concentration and addition of substrate on NO recombination in the following proteins; dehaloperoxidase (6x His DHP), horse heart myoglobin (HHMb) and the H64V mutant of sperm whale myoglobin. The NO recombination experiments allowed us to study and identify protein dynamics involved in the recombination of diatomic ligands to the heme group of myoglobin and dehaloperoxidase.

## 5.2 Methods

Samples were prepared in a 1 mm quartz cuvette with a final buffer concentration of 100 mM potassium phosphate pH 7.0, 120 μM protein, and varying amounts of glycerol. The glycerol concentrations were 0%, 50% and 90% (w/v). Samples that contained 2,4,6-tribromophenol were made by addition the tribromophenol to the buffer at a final concentration of ~1.2 mM. The glycerol was purged with nitrogen gas for several hours to remove oxygen. Addition of a trace of 1M sodium dithionite was used to remove oxygen from the protein and buffer. NO was added to samples by reducing $NO_2$ solutions with trace amounts of 1 mM sodium dithionite. After the NO was added to the protein, samples were allowed to equilibrate several hours to insure proper mixing. Data was collected at the Laboratorie d'Optique et Biosciences located in Palaiseau, France by Scott Brewer and Marten Vos.

## 5.3 Results and Discussion

The absorption spectra of DHPNO and of H64VNO consisted of a weak Q-band absorption and an intense Soret band. Following excitation of either DHPNO or H64VNO with a 550 nm pulse, the Soret band absorption maximum underwent a shift that reflected

photolysis of the NO ligand. In the difference absorption spectrum the photolysis led to a negative feature, or bleach, near 420 nm and a positive feature, or anti-bleach, near 438 nm (see figures 5.1 and 5.2).

Figure 5.3 – 5.6 showed the effect of glycerol on the ligand rebinding kinetics of DHPNO and H64V as well as the effect of substrate on a 0% glycerol sample of DHP. The addition of 2,4,6-tribromophenol to the DHP 0% glycerol samples showed that the substrate has the same kinetics as 50% glycerol does on the ligand rebinding in the DHP. Both glycerol and substrate accelerated the geminate and bimolecular rebinding of the NO ligand. The same kinetic effect was observed for H64VNO samples.

Figure 5.7 and 5.8 showed the time dependence of the differential absorption of signal measured at 438 nm following photolysis of DHPNO and H64VNO. Data were shown for 90% glycerol samples for both proteins and the double exponential fits of the data. Table 1 shows a summary of the double exponential fits like the ones in figure 5.7 and 5.8. The fitted data was time vs. absorbance at 438 nm.

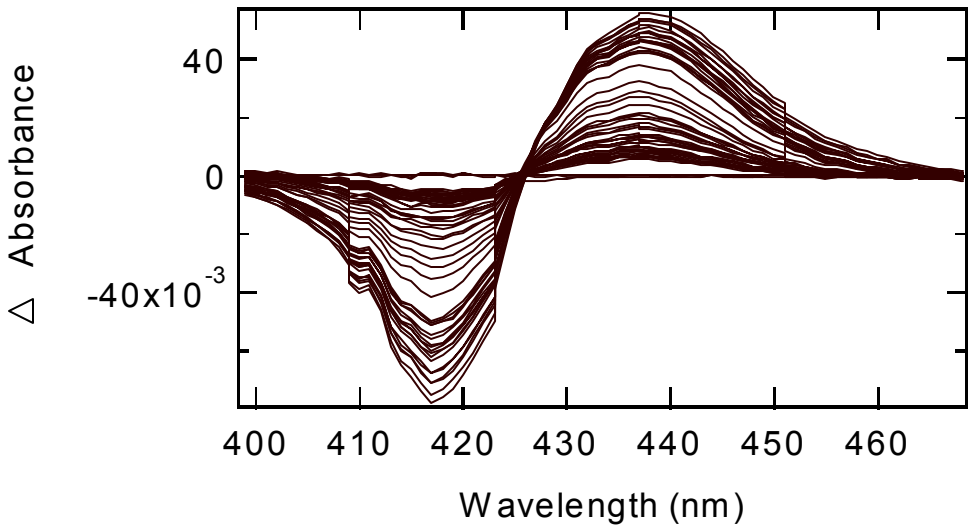


Figrue5.1. the difference spectrum obtained from DHPNO 0% glycerol as a function of a delay time following photolysis. The positive peak at 438 nm results from the Soret band absorption of deliganded DHP, formed upon photolysis whereas the negative peak at 417 nm rests from the disappearance of the Soret band absorption of DHPNO.

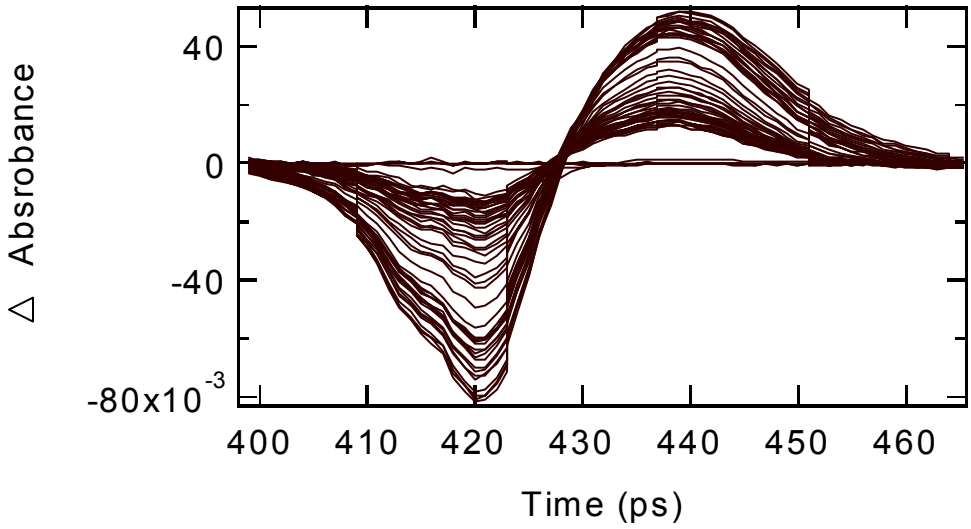


Figure 5.2. The difference spectrum obtained from H64VNO 0% glycerol as a function of a delay time following photolysis. The positive peak at 439 nm results from the Soret band absorption of deliganded H64V, formed upon photolysis whereas the negative peak at 420 nm rests from the disappearance of the Soret band absorption of H64VNO.

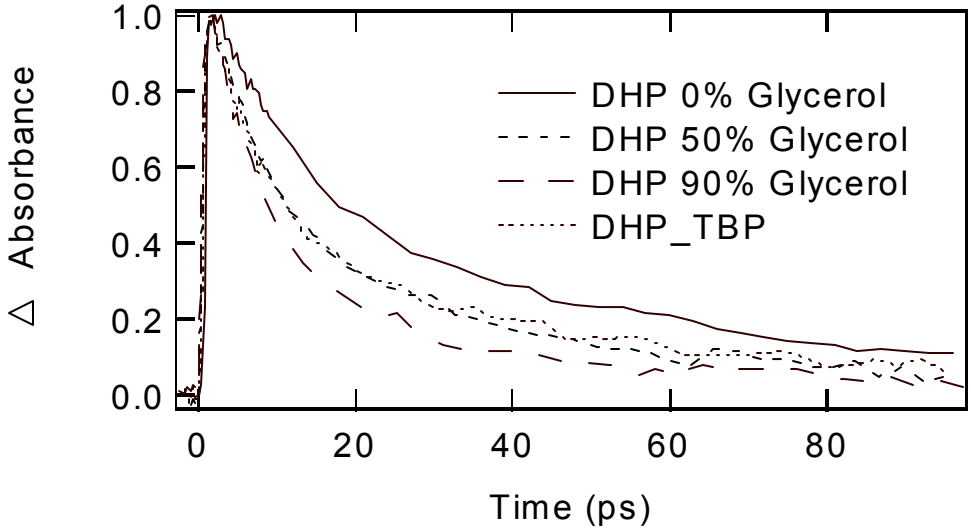


Figure 5.3. The time dependence of the differential absorption signal measured at 438 nm following photolysis of DHPNO. Data are shown for three different glycerol concentrations (w/v) in buffer and the effect substrate has on a 0% glycerol sample.

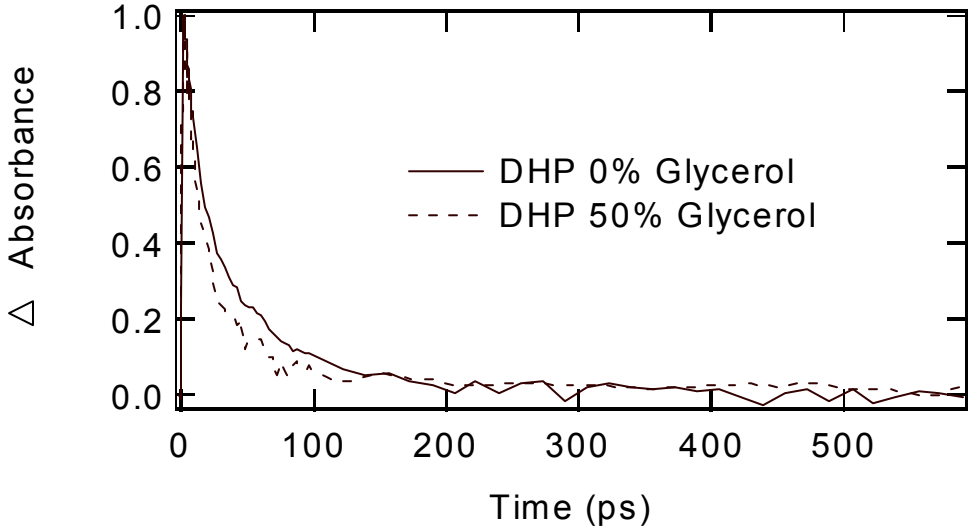


Figure 5.4. The time dependence of the differential absorption signal measured at 438 nm following photolysis of DHPNO. Data are shown for different glycerol concentrations (w/v) in buffer. Extended time range was necessary to allow the signal to return to zero.

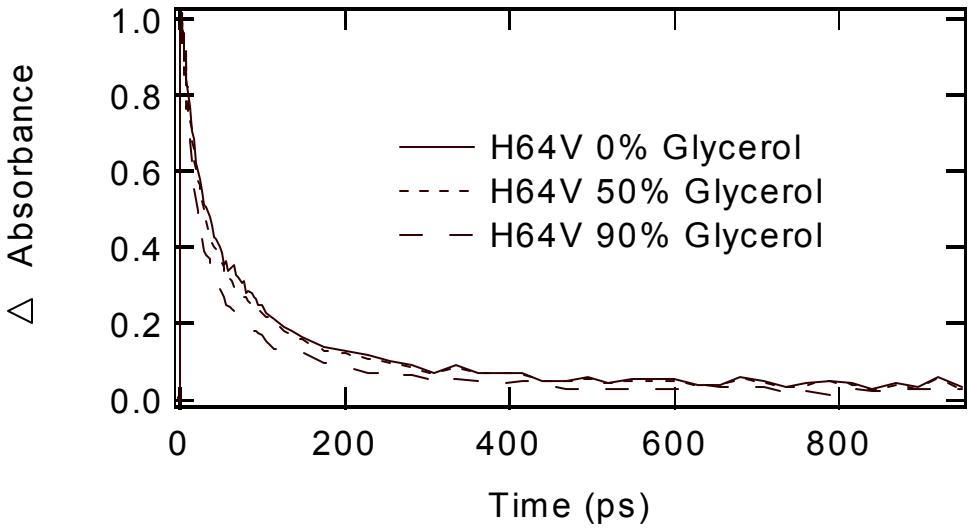


Figure 5.6. The time dependence of the differential absorption signal measured at 438 nm following photolysis of H64VNO. Data are shown for different glycerol concentrations (w/v) in buffer. Extended time range was necessary to allow the signal to return to zero.

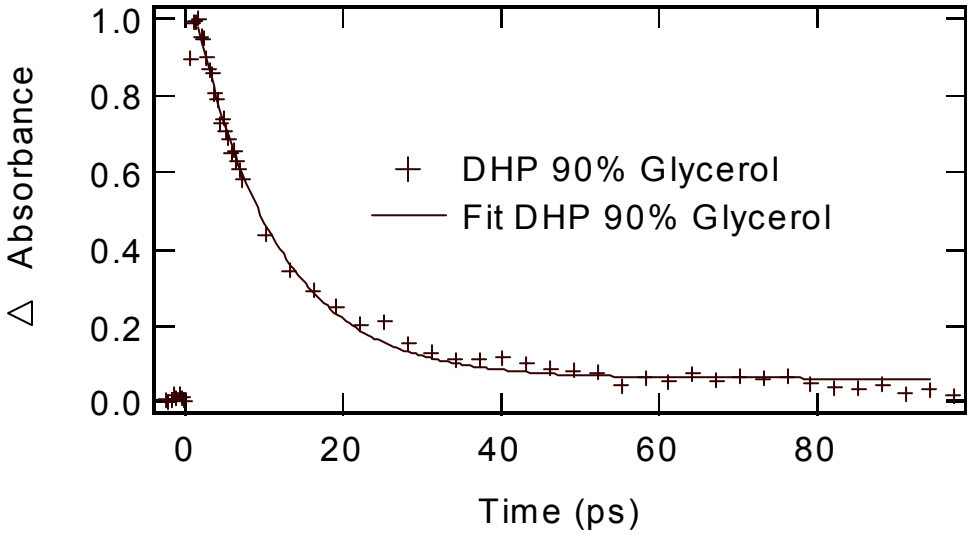


Figure 5.7. The time dependence of the differential absorption of signal measured at 438 nm following photolysis of DHPNO. Data are shown for 90% glycerol and the exponential fit of the data.

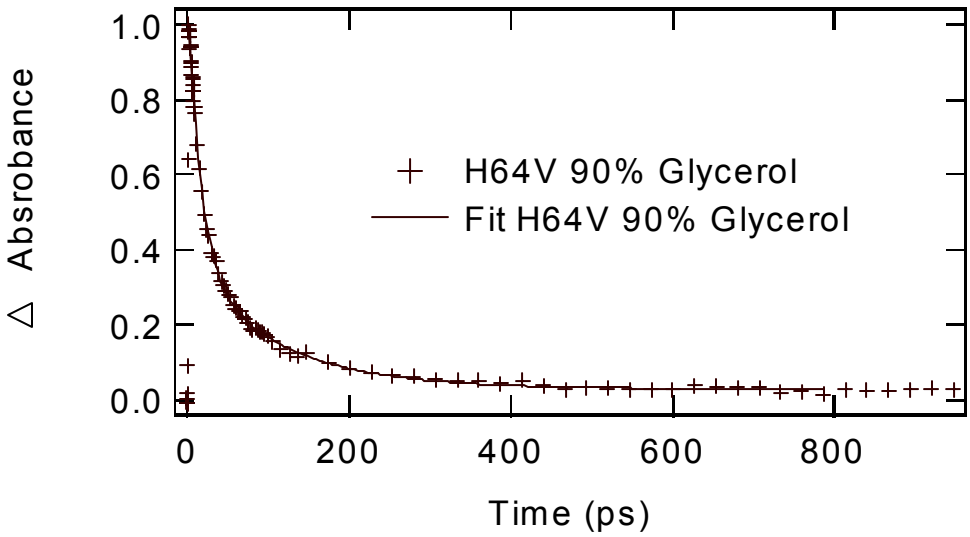


Figure 5.8. The time dependence of the differential absorption of signal measured at 438 nm following photolysis of H64VNO. Data are shown for 90% glycerol and the exponential fit of the data.

| Protein – NO Samples | Rate Constant (ps) | Δ Amplitude |
|---|---|---|
| | | |
| DHP Buffer | 12, 61 | 64, 49 |
| DHP 50% Glycerol | 9.2, 59 | 80, 36 |
| DHP 90% Glycerol | | |
| DHP Buffer + Substrate (TBP) | 6.9, 39 | 71, 43 |
| | | |
| H64V Buffer | | |
| H64V 50% Glycerol | 2.4, 18 | 64, 42 |
| H64V 90% Glycerol | 16.5, 111 | 74, 33 |

Table 5.1. shows the values for rate constant (ps) and Δ amplitudes that were generated from double exponential fits of time vs. absorbance at 438 nm data.

**5.4 Conclusions**

The transient absorption experiments in this chapter have shown that the substrate slowed the protein dynamics thus speed up the rebinding kinetics of NO. The protein dynamics that are most greatly affected are on the distal side. Both substrate and ligands bind on the distal side of the heme. A single exponential cannot describe the dynamics of NO ligand rebinding to the heme group of Mb[1]. The non-exponential character of NO could arise

from distal and/or proximal effects. The proximal model suggests that iron displacement occur on a time scale similar to that of NO recombination, which means the barrier to NO recombination changes with time[3-5]. The distal model suggests that distal residue, valine for DHP and H64V but a histidine for wild type myoglobin, restricts where the NO can diffuse to once photolyzed. In the case of DHP and H64V, the valine allowed for a greater displacement of the photolyzed NO since the pocket was larger. According to the distal side model the histidine restricts the photolyzed NO by caging in the docking site[2].

Transient absorption data from the buffered DHP sample with substrate shows identical kinetics as the 50% glycerol DHP sample, thus supporting the distal model. From X-ray crystal structure of DHP with 4-iodiophenol bound shows that the substrate binds to the distal side of the heme therefore, affects due to addition of substrate probes the distal side of the heme.

Future experiments such as Time-resolved Resonance Raman experiments on these samples will allow us to observe whether there is a correlation between the time scale for the iron out-of-plane displacement and the recombination kinetics of NO. If no correlation exists between the two then it would support the distal controlled model. By including the myoglobin mutant H93G and the DHP mutant H90G in the above experiments we could probe the proximal effects further. Using H93G and H90G mutants will be particularly interesting since the 5- coordinate NO adduct can be probed in the TRRR experiment. The photolyzed 6-coordinate NO adduct results in a 5-coordinate heme iron with an iron-axial-ligand stretching vibration. The photolyzed 5-coordinate NO adduct results in a 4-coordinate species that has no axial ligand mode and characteristic heme Raman bands. Using the combination of the TRRR experiment and time-resolved absorption we hope to determine the

non-exponential charter is due to the distal behavior, which would explain the protein dynamics in the case of NO.

## References:


1. Ye, X., Demdov, A., Champion, P. (2002). Measurements of the Photodissociation Quantum Yields of MbNO and $MbO_2$ and the Vibrational Relaxation of the Six-Coordinate Heme Species.*JACS*. **124**, 5914-5924
2. Franzen, S.; Bohn, B.; Poyart, C.; DePillis, G. D; Boxer, S. G.; Martin, J-L. (1995). Functional Aspects of Ultra-Rapid heme Doming in Hemoglobin, Myoglobin, and the Myoglobin Mutant H93G. J. Biol. Chem. **270**, 1718-1720
3. P. K. Chowdhury, S. Kundu, M. Halder, K. Das, M. S. Hargrove, and J. W. Petrich. (2003). Effects of distal pocket mutations on the geminate recombination of NO with leghemoglobin on the picosecond timescale. J. Phys. Chem. B. 107, 9122-9127
4. Suman Kundu, Barry Snyder, Kaustuv Das, Pramit Chowdhury, Jaehun Park, Jacob W. Petrich, and Mark S. Hargrove, (2002). The leghemoglobin proximal heme pocket directs oxygen dissociation and stabilizes bound heme. Proteins. 46, 268
5. M. Halder, K. Das, P. K. Chowdhury, S. Kundu, M. S. Hargrove, and J. W. Petrich. (2003). A comparative femtosecond study of the unligated monomeric hemeproteins myoglobin and leghemoglobin. J. Phys. Chem. 107, 9933-9938